Available at www.sciencedirect.com

ScienceDirect

journal homepage: www.elsevier.com/locate/watres

Review

Dissolved air flotation and me

*James K. Edzwald**

Department of Civil and Environmental Engineering, University of Massachusetts, Amherst, MA 01003-9293, USA

ARTICLE INFO

Article history:
Received 22 October 2009
Received in revised form
21 December 2009
Accepted 23 December 2009
Available online 6 January 2010

Keywords:
Air bubbles
Coagulation
Dissolved air flotation
Drinking water
Models
Particles
Pathogens

ABSTRACT

This paper is mainly a critical review of the literature and an assessment of what we know about dissolved air flotation (DAF). A few remarks are made at the outset about the author's personal journey in DAF research, his start and its progression. DAF has been used for several decades in drinking water treatment as an alternative clarification method to sedimentation. DAF is particularly effective in treating reservoir water supplies; those supplies containing algae, natural color or natural organic matter; and those with low mineral turbidity. It is more efficient than sedimentation in removing turbidity and particles for these type supplies. Furthermore, it is more efficient in removing *Giardia* cysts and *Cryptosporidium* oocysts. In the last 20 years, fundamental models were developed that provide a basis for understanding the process, optimizing it, and integrating it into water treatment plants. The theories were tested through laboratory and pilot-plant studies. Consequently, there have been trends in which DAF pretreatment has been optimized resulting in better coagulation and a decrease in the size of flocculation tanks. In addition, the hydraulic loading rates have increased reducing the size of DAF processes. While DAF has been used mainly in conventional type water plants, there is now interest in the technology as a pretreatment step in ultrafiltration membrane plants and in desalination reverse osmosis plants.

Contents

* 4 Hillcrest Drive, Potsdam, NY 13676, USA. Tel.: + 1 315 261 4186.
E-mail address: edzwald@ecs.umass.edu

0043-1354/$ – see front matter © 2009 Elsevier Ltd. All rights reserved.
doi:10.1016/j.watres.2009.12.040

1. Introductory remarks

If I have seen a little further it is by standing on the shoulders of Giants. Isaac Newton

The readers of the journal appreciate that researchers stand upon the shoulders of those who came before them. The foundation of our contributions lies with others; *we are a community of scholars*. This is true here. Thus, a better title of the paper would be to replace *and me* with *a not so personal journey*. A major part of my research journey occurred while serving as a professor where I had the good fortune to work with many outstanding graduate students who participated and contributed to the research on dissolved air flotation (DAF), often to a greater extent than I. A philosophy I tried to follow was to base my research on sound scientific principles and to apply them to important applications in providing safe drinking water. The applied research studies led me to work with professionals at water works, consulting engineering firms, and process engineering companies. These folks contributed greatly to the journey.

This was not an easy paper to write. As scientists we are educated to describe our research in an objective, non-personal way. To add personal material is foreign to my nature. I therefore present in Section 1.1 a brief accounting of how I got started on DAF research, mention briefly some key research projects in my career, and identify some colleagues who helped me on my research journey. The remainder of the paper deals with the primary objective of the paper, which is to provide a scientific review of DAF. I have tried my best to be critical and objective of what we know about the subject, but it is my evaluation of the topic and so some of the material reflects my interpretation and assessment. I begin with Section 2 which contains a description of DAF and developments in its use for drinking water treatment. I then proceed with a scientific review of the following subjects: Section 3 on

fundamentals pertaining to air bubbles and the bubble suspension; Section 4 on principles pertaining to particle collisions and attachment to bubbles in the contact zone; Section 5 on principles on rise velocities and separation zone clarification performance; Section 6 on laboratory, pilot-scale, and full-scale plant experience pertaining to performance in treating various water types and integration of DAF into a water plant; and Section 7 on the state of the technology. In some sections I begin with some brief personal comments or reflections, and then I proceed to present an objective review of significant contributions to the topic and what I think is important. I end the paper with a presentation and discussion of research needs in Section 8.

1.1. *A not so personal journey*

I was a graduate student in environmental engineering at the master's level in the mid 1960s at the University of Maryland and studied for the PhD at the University of North Carolina in the late 1960s and early 1970s. We studied the principles and applications of physical–chemical processes (sometimes called unit operations) and flotation was not part of these courses. All instruction on particle clarification was restricted to sedimentation. In classes covering biological processes, there was brief coverage of flotation dealing with vacuum flotation for sludge thickening. I read some literature on flotation clarification processes, but I held the opinion that flotation had no application to clarification of drinking waters and flotation applications were limited to the mining industry and to certain industrial wastewater treatment applications. I was wrong. It turns out DAF was being used in Scandinavia for drinking water treatment since the 1960s, and there is some evidence of earlier use – more on this in Section 2.2.

In 1974 I took a faculty position at Clarkson College of Technology (now Clarkson University). I had the great fortune to meet Egon Matejević who is a world-renown colloid and surface chemist. At that time, Egon had completed some research on microflotation. Microflotation differs from DAF in that bubbles are formed by sparging nitrogen (although air can be used) through a fritted glass filter, and ethanol and lauric acid are added to the suspension to aid foam formation and to control bubble size at a relatively small size of about 50 μm. Because of the addition of these chemicals the technology does not have application to drinking water clarification, but nonetheless Matejević et al. had published papers on removing humic acid (Mangravite et al., 1975) and organic colloids (Cassell et al., 1971) from water. This work motivated me to think about flotation as a clarification technology for removing low density particles from water. While at Clarkson my research activities did not deal with flotation, but I made note that when given the opportunity I should study DAF. This soon occurred when I took a position at the University of Massachusetts (UMass) in 1984.

Upon arriving at UMass three events occurred that allowed me to begin research on DAF. First, the Massachusetts Department of Environmental Protection was interested in whether DAF was a viable treatment process because the Town of Lenox (MA, USA) was in the midst of a demonstration project. Second, the United States Environmental Protection Agency (USEPA) was interested in a research project on DAF funded through their Drinking Water Research Division. Third and most important, I was at that time talking to a new PhD student, James P. Malley, Jr., about the subject of DAF for his dissertation research. I wrote a research proposal to the USEPA, and it was funded in 1985 for three years to develop fundamental process principles for DAF and to examine DAF as a process for treating supplies containing algae and humic substances (natural color).

Two professional colleagues at UMass (David Reckhow and John Tobiason) worked closely with me over many years on several DAF research projects. Both provided expert knowledge on the study of DAF as an integrated water treatment process. Reckhow collaborated with me on applied research studies beginning in the late 1980s on Boston's water supply, and our collaboration continued on other numerous fundamental and applied research projects in the 1990s. Tobiason worked with me on numerous fundamental and applied research projects carried out in Sweden and in the USA. I learned much by working with him.

In the late 1980s and early 1990s, I had a research project funded by the AWWA Research Foundation (now the Water Research Foundation). It had two parts: one a fundamental laboratory and pilot-scale study of DAF that examined air requirements as a function of raw water quality and the effect of pretreatment flocculation time on DAF performance, and an applied phase that involved examination of the performance and costs of several DAF plants in Norway, Sweden, and England. This study enlightened me about the European experience and knowledge on flotation. It also opened doors to future collaboration and research with some key people. Jan Dahlquist, a water process engineer, from Sweden (Purac AB) helped me with the evaluation of plants in Norway and Sweden in the above mentioned study, and we worked together on many subsequent research projects. In the early 1990s Tony Amato, a water process engineer, from England (Purac Ltd., now Enpure Ltd.) entered my journey on DAF research. Two important research studies were conducted first in Sweden and then in the USA. The first study examined pretreatment flocculation effects on DAF and was funded by Anglian Water, Purac AB and Purac Ltd., and the Swedish Government with technical and facility support from Torsten Hedberg at Chalmers University. The second study was done in the USA using pilot-scale facilities set-up in Newport News, VA and Fairfield, CT. We examined high rate flotation and integration with flocculation and filtration. It was funded by Purac Ltd. and Anglian Water. These studies provided significant knowledge to my understanding of DAF, and they were fun working with Jan Dahlqusit, Tony Amato, and my UMass colleague, John Tobiason.

For about 20 years, I had the opportunity to do research on many water treatment projects collaborating with Howard Dunn and Gary Kaminski. Their direct participation and interest in the research contributed to the success of the work. The research began with them at one private water utility (South Central Connecticut Regional Water Authority) and continued at a second one where most of the research was done, the Aquarion Water Company of Connecticut (formerly called BHC). The outcome of several of these projects allowed Aquarion to commission four full-scale DAF plants. The first large facility in Fairfield (CT) is a 190 Ml/

d (mega liters per day) plant and was commissioned in 1997. Another large plant was commissioned in 2007 and is a 115 Ml/d plant in Stamford, CT.

Another key figure in my journey of knowledge on DAF is Professor Johannes Haarhoff. I met him in the early 1990s (at that time he was at Rand Afrikaans University in South Africa, now the University of Johannesburg) at an international conference on flotation in Orlando (Florida) and on a visit by him to UMass in Amherst. Shortly thereafter, Professor Haarhoff spent 1997 on sabbatical leave with me at UMass that led to collaboration on several projects that continues to this day.

I would be remiss not to acknowledge my graduate students who carried out the research and from whom I learned much. I acknowledge them here collectively for their contributions and by name in the Acknowledgements section at the end of the paper.

2. Description and use

2.1. *General description of a dissolved air flotation water plant*

I describe a dissolved air flotation plant so that I may provide some brief background material for the review and to define some terminology. DAF is a clarification process that can be used to remove particles in membrane plants or in conventional type plants using granular media filtration – see top part of Fig. 1. The latter is the most common type of DAF application and is the main focus throughout this review. Discussion of other applications and research needs is covered at the end of the review. It is essential to understand that DAF removes particles that were initially present in the source water supply, those added (e.g., powdered activated carbon (PAC)), those produced via coagulation prior to DAF (mainly precipitated metal hydroxides from coagulation and precipitated natural organic matter (NOM)), and those from oxidation processes (precipitation of Fe and Mn). In a later section, DAF treatment removal efficiency is reviewed for turbidity, algae, *Giardia* and *Cryptosporidium*.

The DAF tank is divided into two zones as indicated in the bottom part of Fig. 1. The front end is called the contact zone. A baffle divides it from the separation zone. The purpose of the contact zone is to provide opportunity for collisions and attachment among floc particles and air bubbles. Air bubbles with attached flocs are called floc–bubble-aggregates. The water carrying the suspension of floc–bubble aggregates, free bubbles, and unattached floc particles flows to the second part of the tank, the separation zone. Here, free bubbles and floc–bubble-aggregates may rise to the surface of the tank. The float layer at the surface of the tank consists of a mixture of

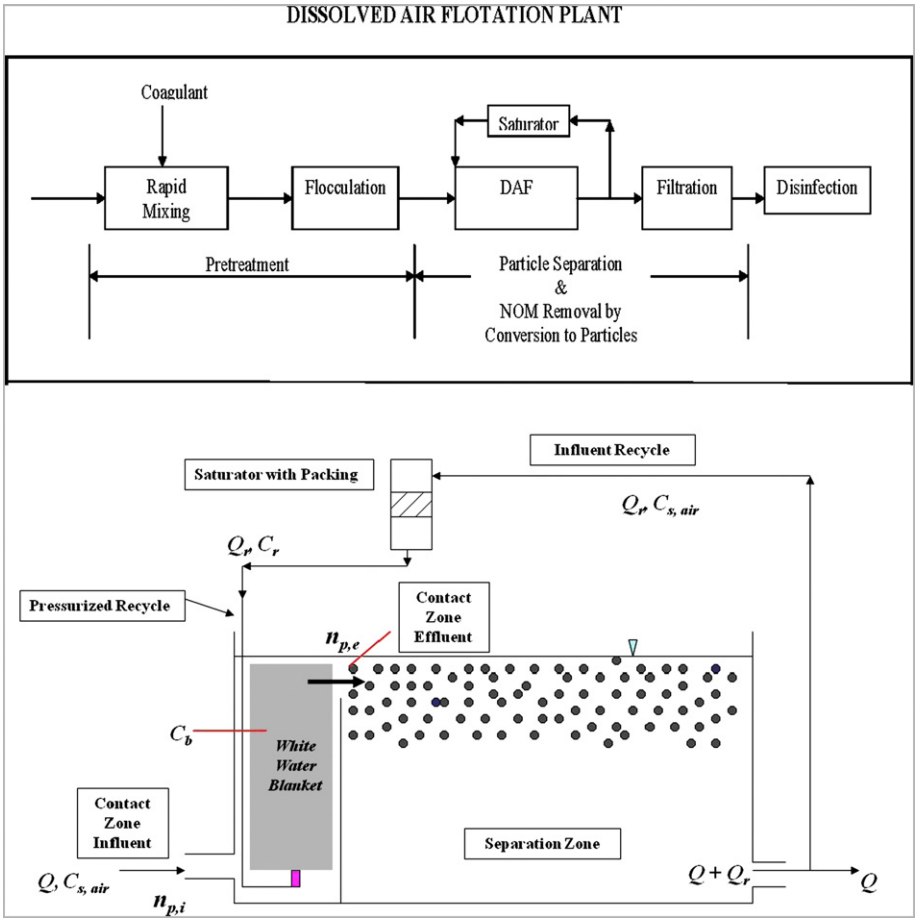

Fig. 1 – Top: Schematic process diagram for a conventional DAF plant. Bottom: DAF tank showing the contact and separation zones.

bubbles and floc particles attached to bubbles. In drinking water applications, this froth is called the float. Over time, this float layer is concentrated producing a sludge that is collected and removed from the tank. Clarified water, often referred to as the subnatant, is withdrawn from the bottom of the tank. In a standard type DAF water plant as presented in the top of Fig. 1, granular media filtration is placed in a horizontal footprint following DAF, and the recycle flow (Q_r) is taken after DAF as shown or after filtration. In some applications, DAF is placed vertically above the filters where the recycle flow is taken after filtration.

Air bubbles are introduced into the DAF contact zone. First, air is dissolved into the recycle flow by adding air under pressure in a vessel called a saturator or air dissolving vessel. Thus, the total amount of air delivered to the contact zone depends on the saturator pressure and the recycle flow. A typical saturator pressure is 500 kPa (72.5 psi). The recycle flow can be described in terms of the recycle ratio or rate (R), which is the recycle flow (Q_r) divided by the plant through-put flow (Q). A typical recycle rate is 10%.

The recycle flow is injected through nozzles or special valves at the bottom entrance to the contact zone. Microbubbles are produced with sizes between 10 and 100 μm. These small air bubbles give the water a milky appearance, and so the term *white water* is used to describe the bubble suspension in the DAF tank.

Analogous to sedimentation overflow rates, DAF tank hydraulic loadings are used to describe the rate and size of DAF tanks. There are conventional DAF processes designed at nominal hydraulic loadings of 5–15 m/h. More recently, high rate DAF processes have been developed at loadings of 15–30 m/h and greater. Loading rates and the development of high rate DAF processes are reviewed further in subsequent sections.

2.2. *Developments*

This section begins with a brief history of the development and use of DAF for drinking water treatment. Some key references are provided so that the interested reader can delve deeper into the material. The section ends with a brief presentation of important trends that have occurred over the last 20–25 years. Some of the developments are continuing and are examined in the scientific review in subsequent sections.

2.2.1. *Brief history of development and use*

DAF as a drinking water clarification method began much earlier than people realize. A vacuum system was used during the 1920s and at least two of these plants were still operating in Sweden in the 1970s (Haarhoff, 2008). In the 1960s DAF as we know it, with pressurized recycle for production of air bubbles, was examined in Finland and Sweden. These DAF systems used higher hydraulic loading rates of 5–10 m/h and deeper tanks than the vacuum systems. Sweden had pressurized type DAF plants in operation beginning in the 1960s. Finland had its first plant in 1965 and by the 1970s DAF was the primary clarification method for treating surface waters rather than settling (Heinänen et al., 1995; Haarhoff, 2008). Numerous plants were built beginning in the late 1960s and continuing since then in Sweden, Finland, and Norway.

In the 1960s there were extensive studies done on DAF in Namibia and South Africa. A wastewater reclamation plant was completed in 1968 in Windhoek (Namibia) in which DAF is used for potable water reuse (Haarhoff, 2008). A new plant using DAF was completed in 2002. Some early fundamental research was done on DAF at the University of Cape Town (Bratby and Marais, 1975a,b). The initial interests in South Africa were about DAF for treating sewage effluents and for thickening, but by the late 1970s DAF was examined to treat eutrophic water supplies culminating with construction of several plants in the 1980s (Offringa, 1995). Extensive documentation of DAF and valuable design guidance based on the South African experience in the 1980s and early 1990s are found in a report by Haarhoff and van Vuuren (1993). These authors subsequently summarized the design parameters from the report in a published paper (Haarhoff and Van Vuuren, 1995).

The Water Research Centre in England began extensive laboratory and pilot-plant studies on DAF in the early 1970s (Gregory, 1997). These studies were practical in nature; they demonstrated the efficiency of DAF to treat algal-laden waters and low turbidity waters containing natural color; they made comparisons to settling; and they developed design and operating criteria that were incorporated into DAF plants in Great Britain in the 1970s and 1980s (Longhurst and Graham, 1987; Gregory, 1997).

The experience with DAF in the Netherlands is documented by van Puffelen et al. (1995). There are several DAF plants in the Netherlands that are used primarily in treatment of algal-laden waters with the first DAF plant in the Netherlands dating from 1979.

DAF is now used widely around the world as noted in the last two international conferences held in Helsinki in 2000 and Seoul in 2007 – see Kiuru and Vahala (2000) and Edzwald and Han (2007). Haarhoff (2008) estimated 60 large DAF plants (50 Ml/d or larger) in 18 countries. Many of these plants are in Canada and the United States (USA).

The application of DAF to drinking water began in the USA in the 1980s. The first plants utilized technology from the Krofta Engineering Corporation. The first plant went on-line as a demonstration plant in 1982 in Lenox, MA (Edzwald et al., 1994). It was replaced by a new and permanent facility in 1994. Two of the Krofta type plants were commissioned in the winter of 1986–1987 in Pittsfield, MA; one of the plants has a fairly large capacity of 90 Ml/d. The Krofta plants are not standard type DAF plants in that all processes are packaged into 1 unit – flocculation, clarification, and filtration – and use low loading rates and high recycle rates. The first DAF plant to use European based design and operating concepts was commissioned in 1993 – Millwood plant at New Castle, NY (Nickols et al., 1995). Canada built its first DAF plant in 1996 at Port Hawkesbury, Nova Scotia. Now there are some 30 DAF plants in the Maritime Provinces of Canada alone. Some large DAF plants were scheduled to go on-line in late 2009 including the 400 Ml/d plant for Winnipeg. I estimate there are now150 DAF plants in the USA and Canada. In the USA there are at least 16 large plants with capacity of 50 Ml/d or greater. A new plant for New York City is under construction with a plant capacity of 1100 Ml/d.

2.2.2. Trends in DAF

In the last 20–25 years there have been significant developments in DAF coupled with a general acceptance of the process by the water supply field. Regarding the latter point, Haarhoff (2008) makes a case that DAF has moved from a developing technology status held up until the 1980s into an accepted one by the mid 1990s as evidenced by DAF being adopted by large water utilities. During this period there were major advances in the science and engineering (technology) of DAF. The science has contributed to our fundamental understanding of DAF. Technological developments have seen a major reduction in the pretreatment flocculation times and an increase in the hydraulic loadings as shown by Fig. 2. Flocculation times have decreased from about 20 to 30 min used early on and into the 1980s to about 10 min now. In some cases even lower flocculation times are used. For example, the Croton water plant under construction for New York City is designed for a flocculation time of 5 min (Crossley and Valade, 2006; Crossley et al., 2007). In the last 10 years or so, there has been the development of high rate DAF systems. Conventional rate DAF is now considered to have hydraulic loadings of 5–15 m/h, and was used exclusively until the late 1990s. It is still used, but high rate DAF is an alternative and has hydraulic loadings of 15–30 m/h and greater. There is extensive coverage later in the paper on conventional and high rate DAF systems. Both scientific research and engineering advances in the process equipment have contributed to these developments of decreasing flocculation times and increasing hydraulic loading rates.

3. Fundamentals pertaining to air bubbles and the bubble suspension

The best things come with bubbles! James K. Edzwald

I often begin oral presentations on DAF with a slide showing pictures of bubbles arising from carbonated soft drinks, beer, Champagne, and dissolved air flotation. This is meant to get the audience's attention to the significance of bubbles in everyday life and in drinking water treatment. In this section material is presented on the solubility of air, bubble properties including shape, size, and charge, and bubble concentrations in the contact zone. My understanding of these subjects was greatly influenced by a book and by Johannes Haarhoff from South Africa. The book is *Bubbles, Drops, and Particles* (Clift et al., 1978). It is an essential reference that lays out the fundamentals of bubble formation, shapes, sizes, and rise velocities. Johannes Haarhoff (University of Johannesburg) is an expert on many DAF subjects including the dissolution of air in saturators, saturator efficiency, and the effects of nozzle design on bubble sizes. He has influenced me greatly, and these topics are covered in this section.

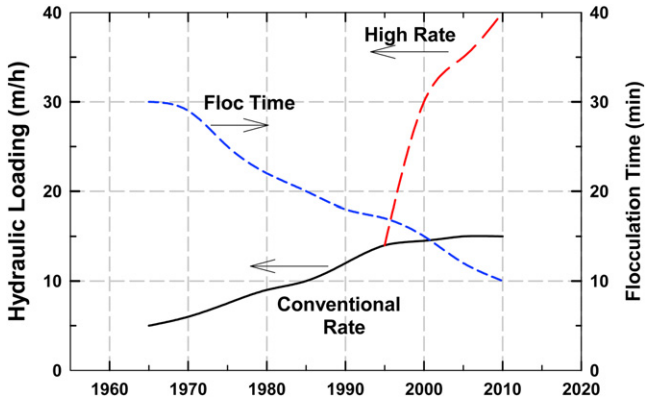

Fig. 2 – Trends in pretreatment flocculation time and DAF hydraulic loading.

3.1. Solubility of air

In DAF processes, we must distinguish between the solubility of air in water under conditions of atmospheric air composition and the solubility of air in the recycle water within the saturator in which the air has a different composition than atmospheric air – saturator air becomes enriched with nitrogen.

3.1.1. Solubility of air in water for atmospheric air composition

The influent recycle water entering the saturator (see $C_{s,air}$ in Fig. 1) is normally in equilibrium with atmospheric air. $C_{s,air}$ is calculated using Henry's law accounting for the fact that air is a mixture of gases. Thus, the solubilities of individual gases are determined and then summed. $C_{s,air}$ is about 24 mg/L at 20 °C increasing to about 32 mg/L for water at 5 °C. Tabulated values as a function of temperature are found in Edzwald (2007a).

3.1.2. Solubility of air in the recycle water exiting the saturator

Oxygen is more soluble in water than nitrogen so within the saturator a steady state condition is established with saturator air containing more nitrogen than atmospheric air. Two important papers on the composition of air in the saturator are those by Haarhoff and Steinback (1996) and Steinback and Haarhoff (1998). They present a kinetic model that predicts the saturator air composition. Several variables affect the kinetics but important ones are the saturator liquid loading rate, saturator pressure, and saturator efficiency. With start-up of saturators, the time to reach a steady state air composition can take several hours. For saturator pressures of 500 kPa and greater, liquid loading rates of 10–15 kg m^{-2} s^{-1}, and saturator efficiencies of at least 80%, steady state air composition is achieved in about 4 h or less. The change in air composition in the first several hours is more important in pilot-scale and laboratory systems, which are not operated continuously. For full-scale plants with continuous saturator operation, it is the steady state air composition (composition of the air within the saturator at equilibrium with water exiting the saturator) that is of interest.

The steady state model for air composition is described by Haarhoff and Steinback (1996) and Steinback and Haarhoff (1998). The steady state air composition depends on the kinetic variables listed above as well as the Henry's constants for

nitrogen and oxygen, temperature, and the oxygen saturation level of the recycle water entering the saturator. The steady state fraction of nitrogen varies only from about 85 to 87% – higher percentage for greater saturator pressure, saturator efficiency, liquid loading rate, and temperature. The saturator air composition at say 86% nitrogen is much greater in nitrogen compared to atmospheric air at about 78%. Since nitrogen is less soluble than oxygen, the pressurized recycle water contains less dissolved air than it would if the saturator could be operated under conditions of maintaining atmospheric air.

Table 1 summarizes the equilibrium air concentrations for dissolved air exiting the saturator (C_r – see Fig. 1) for a range of saturator pressures and two water temperatures. C_r can range from about 110 to 200 mg/L, but for a typical design saturator pressure of 500 kPa and 20 °C, the dissolved air concentration is 130 mg/L.

The dissolving of air in the saturator has kinetic mass (air) transfer limitations so 100% dissolution is not obtained. Saturator efficiencies for packed saturators (contain plastic packing to increase the kinetics of mass transfer) are in the range of 80–95% for dissolving air, while unpacked saturators have lower efficiencies. In addition there may be a slight pressure drop (head loss) between the saturator and the nozzles injecting the recycle flow into the contact zone thereby reducing slightly the delivered air.

3.2. *Bubble properties – shape and size*

The shape of bubbles is set by their rise velocity and hence the bubble size (diameter) – see Clift et al. (1978). Small bubbles (sizes of several 100 μm and less) rise as rigid spheres. These small bubble sizes apply to DAF and so spherical shapes apply and are used in DAF models. Larger bubbles of about 1–10 mm such as occurs in dispersed air flotation have the shape of ellipsoids. Even larger bubbles (>10 mm) take the shape of spherical caps.

Bubble size is an important property in DAF. It affects the performance of collisions and attachment of particles to bubbles and bubble rise velocity. First, fundamentals are presented on what affects bubble size followed by a survey of measurements reported by several investigators.

Bubbles are formed from cavitation from the pressure drop in the nozzle or injection device. Bubbles first form nuclei and then grow. For homogeneous nucleation the critical bubble diameter (d_{cb}) is predicted from Eq. (1) where σ is the surface tension of water and ΔP is the pressure difference across the injection device such as the nozzle. From Eq. (1), the critical nucleus is less than 1 μm for pressure differences of 400–600 kPa such as found in DAF applications.

$$d_{cd} = \frac{4\,\sigma}{\Delta P} \tag{1}$$

The fundamental dependence of smaller bubble nuclei with increasing pressure difference as shown by Eq. (1) is an important concept. However, the actual bubble sizes in DAF systems are affected by heterogeneous nucleation, bubble growth, the injection flow rate, and the injection device. Saturator pressure and the injection device, especially the type of nozzle are important factors affecting bubble size. Within the DAF contact zone, bubble growth can occur by (1) air uptake from the water, (2) a decrease in hydrostatic pressure as bubbles rise in the flotation tank and (3) coalescence or the merging of bubbles. For DAF applications, coalescence is the most important of these effects.

Table 2 summarizes observations of bubble sizes made by several investigators. Before discussing the data in Table 2, a couple of important things about bubble sizes are noted. Bubble formation occurs in two steps, as noted above, with an initial step of formation of bubble nucleation at small sizes (<1 μm) followed quickly by a growth in bubble size through coalescence. The first step of nucleation is reported to occur at times much less than a second after the start of pressure release (Rykaart and Haarhoff, 1995). The coalescence that occurs through the downstream portion of the nozzle orifice and on impinging surfaces of the nozzle produces bubbles of sizes reflecting the measurements reported in Table 2. Rykaart and Haarhoff (1995) found less formation of macrobubbles (>150 μm) when the impinging surface is located closer to the nozzle. Several conclusions are drawn from the data in Table 2 and from the associated references. First, a range of bubble sizes occurs for the contact zone from about 10 to 150 μm. Second, increasing the saturator pressure produces smaller bubbles, but there is a point of diminishing return for pressures greater than about 350 kPa. Reported bubble sizes above 350 kPa saturator pressure are of interest since DAF facilities are designed and operated in the range of 400–600 kPa. Third, most bubbles in the contact zone have sizes of 40–80 μm. There is some growth in the sizes of bubbles as they rise from the bottom of the tank to near the top in moving to the separation zone, but the growth is small. Leppinen and Dalziel (2004) in full-scale plant measurements found bubbles of about 40–80 μm over the depth of the contact zone. Fourth, the bubbles in the separation zone are a little larger than in the contact zone – see Table 2. Leppinen and Dalziel (2004) made bubble size measurements as a function of tank length and depth. They found that most bubbles in the separation zone were in the range of 50–150 μm.

An additional comment on bubble size measurement is warranted, and it has to do with the method used. The most common method is image analysis, but other methods include measurement with an electronic particle counter (light blockage instrument) and by calculation using Stokes' law from measurement of rise velocities. Withdrawal of sample for bubble size from the DAF tank can affect the measurements due to changes in sizes from sample handling. *In-situ* measurements are preferred. A recent paper by

Table 1 – Equilibrium dissolved air concentration (C_r) in the recycle water exiting the saturator for saturator air composition.

Saturator pressure (kPa)	C_r (mg/L)	
	5 °C	20 °C
400	144	108
500	172	130
600	202	151

Table 2 – Bubble sizes in flotation systems.

Bubble Sizes (μm)	Conditions or effects	Reference
10–120	Needle valve: most bubbles 40–90 μm; WRC nozzle: most bubbles 20–50 μm	Zabel (1984)
33–75 (median sizes)	Hague nozzle; larger bubbles at a pressure of 350 kPa compared to 500 and 620 kPa	De Rijk et al. (1994)
200 kPa Pressure 82 and 22 (mean and standard deviation) *500 kPa Pressure* 62 and 22 (mean and standard deviation)	Wide variety of nozzles studied; Percentages of large bubbles (>150 μm) were 7.7% for 200 kPa and 3.4 for 500 kPa	Study by Rykaart reported in Haarhoff and Edzwald (2004)
15–85	Mean sizes of ~30 μm for pressures of 350–608 kPa Increasing size for pressures <350 kPa	Han et al. (2002)
Albert plant 70–84 (median: contact zone) 72–145 (median: separation zone) *Graincliffe plant* 40–60 (contact zone) 50–150 (separation zone)	Full-scale plants Observed bubble clusters (large group of bubbles attached to a floc particle)	Leppinen and Dalziel (2004)

Han et al. (2009) discusses the use of *in-situ* measurements using a particle counter.

3.3. *Bubble–bubble interactions and forces*

As discussed above there is coalescence of bubbles in the downstream side of nozzles producing the bubbles sizes commonly found in the contact zone of mainly 40–80 μm. Bubble–bubble forces then prevent further extensive coalescence in the contact zone. There is evidence of some growth in bubble size for bubbles in the separation zone. A general description and discussion of the forces acting between bubbles follow, and it is noted that coverage of these forces lie within the research interests of surface and colloid chemists and little has been done by water engineers to apply what is known directly to the application of dissolved air flotation.

There are four forces or bubble–bubble interactions that affect bubble behavior in terms of coalescence (these forces also affect bubble–particle interaction, which is covered later). The forces are London-van der Waals (written hereafter, simply van der Waals), electrostatic, long-range attractive hydrophobic interaction, and hydrodynamic repulsion. It is noted that the forces can be described conceptually, which aid our understanding, but in some cases quantification of the forces is difficult. Certainly, more research is needed.

In general the van der Waals force between solid particles may be due to (1) permanent dipole forces, (2) induced dipole forces, and (3) instantaneous induced dipole forces (sometimes called the London dispersion forces). For air bubbles, the gases (mainly N_2 and O_2) are non-polar molecules so the molecular interaction has a London-dispersion origin (weakest intermolecular force). An attractive van der Waals force is thought to exist at small separation distances of about 5–10 nm (Craig et al., 1993).

Air bubbles in waters without the addition of chemical coagulants exert a negative charge, i.e., negative zeta potentials are measured. This causes electrostatic repulsive forces between bubbles. The negative zeta potentials are attributed to the accumulation of negatively charged surfactants or aquatic humic substances that concentrate at the bubble–water interface. However even in the absence of surface active agents, negative zeta potentials are reported. Since air is non-polar, it is hypothesized that the negative zeta potentials are caused by smaller anions that reside at the bubble–water interface at a greater concentration than larger hydrated cations – e.g., distilled or deionized water in equilibrium with air would contain primarily the ions of HCO_3^- (size of about 4 Å) and H^+, actually H_3O^+, (size of 9 Å). Bubble zeta potentials have been reported by Han and Dockko (1999) and Dockko and Han (2004). For experiments with distilled water, bubbles have an IEP (isoelectric point, pH of net charge) at pH < 3, and negative zeta potentials of about – 25 mV over the pH range of 6–8.

The charge at bubble surfaces can be changed and made positive. This is common practice in mineral froth flotation with addition of cationic surfactants or polyelectrolytes. Malley (1995) demonstrated this for DAF with the direct application of cationic polymers to recycle water producing positively charged bubbles. More recently Henderson et al. (2008a) added cationic surfactants to the DAF saturator to produce positively charged bubbles for flotation of algae. Han et al. (2006) have shown that positively charged bubbles can be produced from Al and Mg hydroxide precipitates.

A long-range hydrophobic force that is attractive affects bubble–bubble interaction (and bubble–particle interaction). The origin of this force is not understood, but it has been observed and measured and has a range of 150 nm (Israelachvili and Pashley, 1982; Ducker et al., 1994).

There is a structural force that is repulsive in nature – i.e., it inhibits bubble coalescence and bubble–floc attachment. It is the water between bubbles that must be displaced for two bubbles to coalesce or for attachment of a particle to a bubble. This force is called the disjoining pressure by some flotation researchers (e.g., Derjaguin et al., 1984) or hydrodynamic repulsion. In the colloid and filtration fields, it is often referred to as the hydrodynamic force or retardation. Energy is

required for drainage of the intervening water between bubbles. This force is significant at inter-bubble distances of less than 10 nm (Craig et al. (1993)). It is a significant force in inhibiting bubble coalescence, especially for larger bubbles than found in DAF.

Craig et al. (1993) reported, for bubbles larger than found in DAF, that at low salt concentrations there is bubble coalescence and at high salt concentration there is little or no coalescence. This author is unaware of any such studies for small bubbles such as occur in DAF. For most drinking water applications, salt concentrations are low (ionic strength < 0.02 M), and bubble coalescence occurs in the formation of the bubbles as reported in the prior section on bubble sizes. For DAF in pretreatment desalination applications for estuarine and seawaters, ionic strengths are high. The author is not aware of any literature on salt water effects on bubble coalescence, but this is an area that should be investigated and reported.

3.4. *Bubble suspension concentrations in the contact zone*

There are three measures of bubble concentrations: mass, volume, and number. The mass concentration (C_b) is used in design practice and has practical applicability in evaluating the efficiency of delivering air to the contactor. The volume (Φ_b) and number concentrations (n_b) are important theoretical variables in modeling the contact zone performance and in calculating floc–bubble aggregate rise velocities.

The mass concentration (C_b – see Fig. 1) of bubbles in the *white water* bubble suspension, or bubble blanket, in the contact zone is obtained from a steady state mass balance.

$$C_b = \frac{\{e(C_r - C_{s,air})R - k\}}{1+R} \tag{2}$$

The difference between C_r and $C_{s,air}$ represents the amount of air that will theoretically precipitate based on saturation of air in the recycle flow and the influent flow to the contact zone – i.e., released as air bubbles. The dissolved air in the recycle flow entering the contact zone does not reach an equilibrium concentration since the air transfer into water in the saturator has kinetic limitations. There may be a loss in pressure (head loss) between the saturator and the recycle injection point in the contact zone affecting the delivered air. Thus an efficiency factor (e) is incorporated into the mass balance. The parameter, k, accounts for any air deficit in the incoming flocculated water (Q). If the flocculated water is at saturation, then k is zero. This is the common situation, but not always. Waters are usually saturated with nitrogen gas so any air deficit is attributed to oxygen. Supplies taken from the bottom of reservoirs that are mesotrophic or eutrophic, may have an oxygen deficit, and therefore an air deficit.

The air bubble volume concentration in the contact zone (Φ_b) is calculated from Eq. (3). Moist air densities (ρ_b) for conditions of 100% humidity and with the dew point temperature equal to the water temperature are used. Values for ρ_b at 4 and 20 °C are 1.27 and 1.19 kg/m^3. Other values can be found in chemistry handbooks.

$$\Phi_b = \frac{C_b}{\rho_b} \tag{3}$$

The bubble number concentration is calculated from Eq. (4). Measured or assumed bubble sizes are required for calculation of n_b. Ranges in bubble sizes and typical values were presented above in Section 3.2.

$$n_b = \frac{\Phi_b}{\pi(d_b)^3/6} \tag{4}$$

Table 3 presents mass, volume, and number concentrations for recycle rates of 8–12% (practical range for operation) at a fixed saturator pressure of 500 kPa. The information in the table shows that the air bubble mass concentrations (C_b) range from 7 to 10 mg/L, the volume concentrations (Φ_b) are 5900–8600 ppm, and the number concentrations (n_b) are about 50×10^3 to 80×10^3 bubbles per mL. If we examine values for 10% recycle, then we see that there is at least one bubble for every floc particle entering the contact zone as long as floc particle number concentrations are less than 65×10^3 floc particles per mL. Bubble volume concentrations, important in lowering floc density, greatly exceed floc particle volume concentrations. For example, flocs with density of 1100 kg/m^3 at a suspended solids concentration of 110 mg/L yields a floc particle volume concentrations of 100 ppm, which is greater than most DAF applications. Thus, the ratio of bubble volume at 7300 ppm (see Table 3 for 10% recycle) to floc particle volume (100 ppm) is 73. This high ratio insures adequate bubble volume to lower the density of the floc–bubble aggregates to less than the water density, and the aggregates rise to the surface – this is covered in Section 5.

The last column in Table 3 gives the mean separation distance (d_{sd}) between air bubbles in the *white water* blanket or bubble suspension. Values for d_{sd} are about 200 μm. The open space for water between bubbles is roughly at a distance comparable to the pore openings between filter grains in filter beds. This comparison between the *white water* blanket and filters is a feature of interest that is used in one modeling approach for the contact zone that is presented in the next section.

4. Principles pertaining to particle collisions and attachment to bubbles

> Everything should be as simple as it is, but not simpler.
> Albert Einstein

Table 3 – Air concentrations and bubble separation distances versus recycle rate (conditions: 20 °C, saturator pressure of 500 kPa, efficiency of delivering air (e) of 90%, bubble diameter of 60 μm, flocculated water is saturated with air ($k = 0$)).

Recycle rate, R (%)	Mass conc., C_b (mg/L)	Volume conc., Φ_b (ppm)	Number conc., n_b (#/mL)	Mean separation distance between bubbles, d_{sd} (μm)
8	7.1	5900	50×10^3	210
10	8.7	7300	65×10^3	190
12	10.2	8600	80×10^3	180

What I believe Einstein meant is that models whether they be scientific word descriptions or mathematical expressions should include the important variables describing the problem but should not be burdened with unnecessary detail. This is my approach in developing models to describe dissolved air flotation. Models describing collisions of particles to bubbles and their attachment are the subject of this section.

My thinking about how to model bubble–particle interactions and collisions between particles and bubbles was influenced by three papers I read and studied during 1985. None of the papers dealt specifically with DAF, but each paper influenced me. The first paper was by Derjaguin who had a major role in the development of DLVO theory describing colloid stability. His paper is entitled, *Kinetic Theory of Flotation of Small Particles* (Derjaguin et al., 1984). In this paper Dergaguin et al. distinguished between contact flotation and contactless flotation. When bubbles, especially larger ones, attach to large particles (~100 μm and larger) a contact angle can be measured that signifies the particle hydrophobicity and adhesion to the bubble. This applies to large particle and bubble processes such as dispersed air flotation. For small particles and bubbles there are repulsive and attractive forces between particles and bubbles that affect collisions and attachment. Derjaguin et al. explained that the repulsive and attractive forces are important and not a wetting perimeter or contact angle, and called this contactless flotation. For small particles colliding with a rising bubble, the authors described a trajectory for a particle as it moved to and around a bubble affected by long-range hydrodynamic interaction, electrostatic repulsion (for bubbles and particles of same charge), London-van der Waals attractive forces, and a short-range hydrodynamic interaction (water layer at the particle surface).

Two other important papers were those by Flint and Howarth (1971) and Reay and Ratcliff (1973). In these papers the authors examined particle trajectories around rising air bubbles and expressed the collision efficiency in terms of particle transport processes of gravity (inertia, sedimentation, and interception). They related the particle transport processes to the single collector collision efficiency concept. Furthermore, Reay and Ratcliff (1973) used the Stokes–Einstein relationship to come up with a single collector efficiency expression to describe transport of small particles to bubble surfaces by Brownian diffusion. Adhesion (attachment) of particles to bubbles was handled separately through an adhesion efficiency factor. These two important papers led me to develop a modeling approach for the DAF contact zone, analogous to air and water filtration, in which the bubbles are collectors of particles. More on this model under the *white water* bubble blanket modeling approach below.

4.1. *Modeling approaches*

Many researchers have presented models to describe the performance of the contact zone. A summary of contributions to these models is listed in Table 4. This table is referred to throughout this section. Numerous names have been given to these models; however, there are basically two approaches: flocculation type models and *white water* blanket filtration type models. In the flocculation models, collisions are treated in a similar way to heterogeneous based flocculation with particles or flocs colliding with bubbles (in other words, the bubbles are viewed as a group of particles). In the *white water* blanket filtration approach, a blanket of bubbles acts as collectors of particles analogous to the anthracite or sand media in a filter acting as collectors. Both types of models are reviewed and discussed.

All models begin with second order rate kinetics to describe the rate of particle change due to collision and attachment to bubbles.

$$\frac{dn_p}{dt} = -k_c n_p n_b \tag{5}$$

where k_c is the rate coefficient, n_p *and* n_b are the particle and bubble number concentrations, respectively. How this equation is incorporated into two heteroflocculation type models and the *white water* filtration type model is addressed in the next section.

4.2. *Heterogeneous flocculation type models*

4.2.1. *Turbulent flocculation model*

Tambo et al. (Tambo et al., 1986; Fukushi et al., 1995; Matsui et al., 1998) developed a model in which collisions among floc particles and bubbles are brought about by turbulent mixing in the contact zone. The mixing produces velocity gradients causing collisions analogous to what occurs in a flocculation tank. The mixing is characterized in terms of the energy dissipation per contact zone water volume, or practically mixing is described in terms of the root-mean-square velocity gradient, G. The model equations are summarized in Table 4. Eq. (6) is the rate equation that applies to the condition of collisions between flocs without previously attached air bubbles. Tambo uses Eq. (7) to describe collisions between bubbles with flocs containing attached bubbles. In other words as time proceeds, he considers that multiple bubble attachment to large flocs can occur. The maximum number ($N_{b,max}$) of bubbles that can possibly attach to one floc particle depends on the surface areas of the flocs and bubbles. It is calculated from Eq. (8).

The authors have not tested directly their contact zone flocculation based model with experimental data. They have, however, coupled the contact zone model to separation zone rise velocities and compared overall flotation performance with experimental data (Fukushi et al., 1995, 1998). They had some success in confirming overall flotation performance with experimental data collected for suspensions with large flocs of about 100–1000 μm. However, DAF treatment of large flocs has limited application to drinking water treatment. In most drinking water applications, much smaller flocs are produced and floated. There is a considerable body of evidence that the flocs should be much smaller than 100 μm. Optimum floc sizes for drinking water applications of DAF are discussed later.

There are other limitations of the Tambo flocculation based models for the contact zone. First, the only collision mechanism in the model is that from mixing. The authors ignore collisions by other mechanisms such as Brownian diffusion for small particles. Second, the authors model the contact zone in terms of the energy dissipation to the volume of the contact zone. In other words, there is extensive mixing

Table 4 – DAF contact zone models (equation variables defined at end of paper under Equation Notation).

Primary Equations	Model Basis	Comments	Reference
Heterogenous flocculation: turbulent flocculation model			
Rate equation for particles without previously attached bubbles $(dn_{p,o}/dt) = \left[-\ 0.385\ \alpha_{pb}\left(G(d_p + d_b)^3\right) n_b n_{p,o}\right]$ (6)	1. Considers collisions produced by velocity gradient under turbulent mixing. 4. Considers contact zone is mixed.	1. Models are for batch kinetics or batch flotation. 2. To apply to continuous flow DAF, one must incorporate kinetics into CFSTR reactor.	Tambo et al. (1986) Fukushi et al. (1995) Matsui et al. (1998)
Rate equation for particles with previously attached bubbles from i to $N_{b,max}$ $dn_{f,i}/dt = \left[-0.385\alpha_{pb}G(d_f + d_b)^3 n_b \left(\alpha_{pb,i} n_{f,i} - \alpha_{pb,i-1} n_{f,i-1}\right)\right]$ (7)			
$N_{b,max} = \pi(d_f/d_b)^2$ (8)			
For conditions where n_b is in excess and flocs are about the size of the bubbles or smaller $(n_p/n_{p,o}) \cong \exp\left[-0.385\left(\alpha_{pb}G(d_p + d_b)^3 n_b t\right)\right]$ (9)			
Heterogeneous flocculation: particle–bubble trajectory flocculation model			
$E_{pb} = \left(X_c^2/(r_p + r_b)^2\right)$ (10) $(n_p/n_{p,o}) = \exp\left[-\left((r_b + r_p)^2 E_{pb} n_b'\right)\right]$ (11) where n_b' is the bubble number generated per time per area	1. Considers particle trajectory to rising air bubbles. 2. Particle trajectory and capture by bubbles affected by hydrodynamic and interparticle forces. Only particle transport mechanisms of gravity settling and interception are considered.	1. E_{pb} is a calculated from particle trajectory analysis. It is a combined theoretical collision and attachment efficiency coefficient. Used in Eq. (11) to predict the contact zone performance. 2. Eq. (11) is for batch kinetics.	Leppinen (1999, 2000)
$E_{pb} = \left(X_c^2/(r_p + r_b)^2\right)$ (10) flotation rate $\propto E_{pb}\beta_{DS} n_p n_b$ (12) where $\beta_{DS} = (\pi g/72\mu)\left(\rho_p - \rho_w\right)(d_p + d_b)^3 \lvert d_p - d_b \rvert$ (13)	1. Han et al. used a similar particle trajectory approach for calculating E_{pb}. 2. Does not give flotation rate equation, but states it is analogous to flocculation by differential sedimentation. If so, would have rate equation like Eq. (12)		Han et al. (1997) Han (2002)

(*continued on next page*)

Table 4 (continued)

Primary Equations		Model Basis	Comments	Reference
White water *bubble blanket models*				
$\eta_D = 6.18\left[\left(k_b T/g(\rho_w-\rho_b)\right)\right]^{2/3}\left[1/d_p\right]^{2/3}\left[1/d_p\right]^2$	(14)	1. Blanket of bubbles (*white water* blanket) in the contact zone at a dynamic steady state at high bubble number concentration. 2. Bubbles act as collectors. 3. Particle transport terms expressed with respect to the single collector efficiencies. Expressions for interception (η_I), settling (η_S), and inertia (not shown since not important for DAF) developed from particle trajectory analysis. Expression for Brownian diffusion (η_B) obtained from Stokes–Einstein relationship.	1. Performance equation (Eq. (18)) is for continuous steady flow through the contact zone assuming plug flow hydraulics – see text for discussion of plug flow. 2. Interparticle forces attributed to London-van der Waals and electrostatic forces not incorporated into particle trajectory analysis. Short range hydrodynamic effect of water layer between bubble and particle not considered in model. All of these effects are accounted for in the empirical attachment efficiency term, α_{pb}. These forces are discussed in the text.	Edzwald et al. (1990) Edzwald (1995) Haarhoff and Edzwald (2004)
$\eta_I = \left((d_p/d_b)+1\right)^2 - (3/2)\left((d_p/d_b)+1\right) + (1/2)\left((d_p/d_b)+1\right)^{-1}$	(15)			
$\eta_S = \left[\left(\rho_p-\rho_w\right)/\left(\rho_w-\rho_b\right)\right]\left[d_p/d_b\right]^2$	(16)			
$\eta_T = \eta_D + \eta_I + \eta_S$	(17)			
$n_{p,e}/n_{p,i} = \left(\exp\left(-(3/2)\alpha_{pb}\eta_T\Phi_b v_b t_{cz}/d_b\right)\right)$	(18)			

throughout the entire contact zone. The hydraulics of the contact zone is discussed in some detail later in the paper, and it is shown that the contact zone for full-scale DAF tanks is not completely mixed. Third, if one assumes complete mixing, then one cannot use directly the batch kinetic equations (Eqs. (6) and (8)) to model continuous flow full-scale DAF tanks. One must incorporate the equations into a mass balance for a continuous flow stirred tank reactor (CFSTR). Fourth, it is well-known that DAF with small bubbles is a more efficient process than large bubble systems such as dispersed air flotation; in other words, flotation efficiency increases with decreasing bubble size. However, their flocculation model for the conditions described by Eqs. (6) and (7) predict the opposite effect of bubble size. This is because the equations describe second order flocculation kinetics in which the bubble number concentration (n_b) is changing so performance improves as the bubble size gets larger – see Eqs. (6) and (7) dependence on d_b^3.

Tambo considered a modeling case in which the bubble concentration is in excess compared to particle concentrations and in which floc sizes are about that of the bubbles or smaller. The integrated rate equation (Eq. (9)) for this case is presented in Table 4. Note that this is for batch kinetics and not for a flow-through tank. One can show the widely accepted concept that smaller bubbles yield better performance by making modification to Eq. (9). We replace the bubble number concentration (n_b) with a volume concentration (Φ_b), and assume conservation of bubble volume. This results in a bubble size dependence as $(d_p + d_b)^3/(d_b)^3$ in which smaller bubbles increase efficiency. Additional discussion of the effect of bubble size on contact zone performance is covered in greater detail below.

4.2.2. *Particle–bubble trajectory based flocculation models*

This type of modeling approach considers the effects of hydrodynamic interactions and interparticle forces that occur between a rising air bubble and a particle in suspension undergoing gravitational forces. It is analogous to the particle–particle flocculation model called curvilinear flocculation by Han and Lawler (1992). The Tambo model according to the Han and Lawler terminology is a rectangular based model because it ignores deviation in the particle trajectory around rising air bubbles. In some literature the terminology of long-range model is used in place of rectangular and short-range model used instead of curvilinear. Since the separation distance at which particle–bubble forces are important are often referred to as short-range and long-range forces, I use the terminology of rectangular and curvilinear modeling.

The particle–bubble trajectory flocculation modeling approach was used by Leppinen (1999, 2000) and by Han (Han et al., 1997; Han, 2002). Both researchers consider only the collision mechanism of gravity settling of the particle to the bubble, and thus the model is analogous to flocculation by differential settling where hydrodynamic and interparticle interactions are included. They considered larger particle sizes where collisions with bubbles by Brownian motion can be ignored, and they did not consider collisions by fluid shear (turbulent flocculation) as done by Tambo et al. (Tambo et al., 1986; Fukushi et al., 1995; Matsui et al., 1998). As the particle approaches the bubble its flow path deviates around the

bubble due to the water between the particle and bubble – this is called hydrodynamic interaction or sometimes hydrodynamic retardation. At close distances between the particle and bubble there are interparticle (here, particle–bubble) forces. These interparticle forces are attributed to van der Waals forces and electrostatic forces. The van der Waals forces are considered attractive in nature; however, for particle–bubble interactions this may not necessarily be true as explained later. Electrostatic forces may be repulsive, if the particles and bubbles have the same charge (usually negative) or may be attractive if the particle or bubble charge can be altered through coagulation producing opposite charges.

A particle trajectory is calculated considering the above hydrodynamic and interparticle forces to determine the path of particles moving toward and around a bubble. Particles that have an initial separation distance, as depicted for the Curvilinear Model case in Fig. 3, between the particle and bubble of $X < X_c$ collide and attach to the bubble. E_{pb} (Eq. (10), Table 4) is the collision efficiency and is defined as the ratio of the area that leads to collision for the Curvilinear Model particle trajectory case (X_c^2) to the collision area of $(r_p + r_b)^2$ for the Rectangular Model (see depiction in Fig. 3).

Leppinen (1999, 2000) incorporates the collision efficiency term (E_{pb}) into a kinetic rate equation that yields a contact zone performance equation (see Eq. (11) in Table 4) assuming batch kinetics or plug flow for the DAF contact zone. Han's papers (Han et al., 1997; Han, 2002) report only on calculations for E_{pb}. I was unable to find that this term was incorporated into an overall kinetic rate equation such as Eq. (5). If readers delve into the Han papers, note that Han uses a symbol of α for E_{pb}. This has caused confusion in the flotation field because Tambo, Edzwald, and others reserve the notation of α to describe attachment efficiency only. In Table 4, I note that E_{pb} would have to be incorporated into a flotation rate equation (Eq. (12)), and if transport of particles to bubbles occurs by settling the expression for the collision efficiency function (β_{DS}) is shown – see Eq. (13).

Note these authors refer to E_{pb} as a collision efficiency variable; however, it combines both particle transport and attachment. The equations for the hydrodynamic and interparticle interactions that are used to determine E_{pb} are not presented here and so the reader is referred to the papers by Leppinen and Han and to a thorough presentation of the equations by Okada et al. (1990). Basically, what is done is follows. As the particle moves toward a bubble, its flow path deviates around the bubble due the water between the particle and bubble (hydrodynamic force). The particle path is also affected by interparticle forces due to electrostatic effects (repulsion if particle and bubble have same charge and attractive if of opposite charge). In this approach they calculate the forces as a function of distance as a particle passes around the bubble. Repeated trials are made setting an initial separation distance, X, where X_c is the largest separation distance that results in a collision.

Some brief comments and discussion follow. First, the model is difficult to use as a practical tool to predict contact zone performance. Hydrodynamic and interparticle force equations are required to calculate X_c thereby yielding a value for the collision efficiency (E_{pb}) by use of Eq. (10). Second, some of the variables in these equations are more conducive for use in model particle and water systems, but not for actual DAF drinking water applications. For example, to calculate interparticle forces require (1) the Hamaker constant for the type particles under consideration in water interacting with an air bubble, (2) the zeta potentials for the bubbles and particles, and (3) the ionic strength of the water to calculate the inverse of the electrical double layer thickness. To calculate electrostatic forces, the surface potentials of the particles and bubbles are required. These can be calculated from zeta potentials of particles and bubbles, in turn calculated from electrophoretic mobility measurements, but these measurements are difficult to make for bubbles and the measurements are rarely made in practice. For particle–particle van der Waals interaction, similar particles are usually considered and values for the Hamaker constant for the van der Waals force equations are reasonably well-known. For particle–bubble interaction in water we have dissimilar particles and there is much less information on Hamaker constant values especially for real systems involving a mixture of particles (organic and inorganic particles and metal hydroxides precipitate) making up flocs and bubbles. Okada et al. (1990) report a Hamaker constant of 3.54×10^{-20} J for latex particles and air bubbles. Leppinen (2000) in his model arbitrarily assumed a value of 10^{-20} J, while Han (2002) considered a range of values of 3.5×10^{-20}–8.0×10^{-20} J. Air bubbles are non-polar substances so they are in fact much different from solid particles with surface functional groups. For particle–particle interaction in water, the van der Waals force is attractive and a major cause of particle–particle attachment. This is not the case for particle–bubble interaction – it can be attractive or repulsive depending on the solid particle. Ducker et al. (1994) report a negative Hamaker constant of 10^{-20} J for air bubbles and hydrophilic silica. They also point out that the van der Waals force is affected by adsorption of surfactants at the air–water interface. Lu (1991) also makes a case that the London dispersion force for a non-polar bubble and a particle in water is repulsive. In their paper a negative Hamaker constant of 1.4×10^{-20} J was used for a manganese carbonate mineral particle interaction with bubbles.

Third, the model assumes a hydrodynamic force between two rigid solids – i.e., the particles and bubbles are not porous. This assumption for the bubble is actually valid, but flocs contain particle aggregates with water within the aggregate producing porosity. The effect of the floc porosity is to reduce the hydrodynamic particle–bubble force interaction and thus there will be a greater collision efficiency than predicted. This reduced hydrodynamic force due to floc porosity is not considered in the models.

Finally, the dependency of flotation efficiency on bubble size in the Leppinen and Han models is contrary to the fact that flotation efficiency improves with decreasing bubble size. The Leppinen model (Eq. (11)) predicts, through the term $(r_b + r_p)^2$, poorer contact zone performance for decreasing bubble size although it is not clear what the dependency of E_{pb} is with decreasing size. Han (Han et al., 1997; Han, 2002) does not give a flotation rate equation in his papers, but he does say that his modeling approach is analogous to that of flocculation by differential sedimentation. If that is true, Eq. (12) shows the flotation rate and Eq. (13) shows the dependency of the collision frequency factor function on bubble size where it

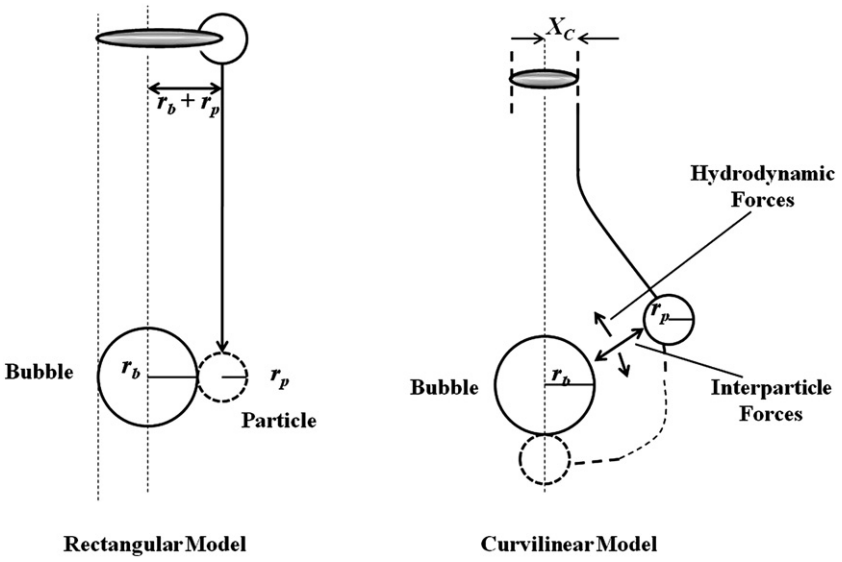

Fig. 3 – Rectangular model depicts particle capture by bubble for particles within critical region of $r_b + r_p$ (no hydrodynamic and interparticle forces; all collisions result in attachment). Curvilinear model depicts particle trajectory of rising air bubble and particle settling affected by hydrodynamic and interparticle forces.

increases with increasing bubble size. This is a flaw in using flocculation based models to describe contact zone flotation performance.

4.3. *White water bubble blanket model*

This modeling approach considers bubbles in the *white water* blanket within the contact zone as collectors of particles using the single collector efficiency approach to account for particle transport to the bubble interface. The *white water* blanket of bubbles exists in the contact zone at a dynamic steady state at a high bubble concentration ($>50 \times 10^3$ bubbles per mL, Table 3). This dynamic steady state is maintained by continuous injection of bubbles from the recycle flow and output at the exit of the contact zone. Details of the model are found in two papers of Edzwald et al. (Edzwald et al., 1990; Edzwald, 1995), and the model was subsequently examined in a review by Haarhoff and Edzwald (2004).

Air bubbles in the *white water* blanket act as collectors of particles or flocs, and the dimensionless particle transport coefficient (η_T) is used to account for the total collision efficiency of a single bubble or collector due to the various transport mechanisms. Collisions may occur by Brownian diffusion (η_D), by fluid flow or interception (η_I), and by settling of flocs (η_S) onto bubbles as depicted in Fig. 4. In this figure the bubble is rising at a velocity (v_b) producing streamlines of flow in the downward direction as shown. These streamlines are characterized by Stokes flow conditions given that the rise velocities of bubbles less than 120 μm have Reynolds numbers <1. The single collector efficiency concept was first used in air filtration models (Friedlander, 1977) and then adapted to model granular media water filtration (Yao et al., 1971). It has also been used by others to describe collection of particles by bubbles in froth flotation (Flint and Howarth, 1971) and in dispersed air flotation (Reay and Ratcliff, 1973).

Eqs. (14)–(16) in Table 4 describe the individual single collector efficiencies. It is noted that the single collector collision efficiency (η_T) does not consider interparticle forces, only particle transport. Whether potential collisions are successful and result in attachment is accounted for by an empirical coefficient, α_{pb} – fraction of successful collisions. This approach differs from the flocculation trajectory approaches of Leppinen (1999, 2000) and Han (Han et al., 1997; Han, 2002) discussed in Section 4.2.2. In the *white water* model, the effect of streamlines of flow diverting around the bubble are considered in the single collector efficiency equations. In fact, the expressions for interception and settling were derived from particle trajectory analysis. The convective-diffusion equation was used to obtain the expression for Brownian diffusion (η_D).

Utilizing the second order rate expression for flotation of Eq. (5) and accounting for the attachment efficiency (α_{pb}) of particles colliding with bubbles, the single collector efficiency (η_T), the volume of suspension swept by a rising air bubble ($v_b(\pi d_b^2/4)$), we get Eq. (5a)

$$\frac{dn_p}{dt} = -\alpha_{pb}\eta_T v_b\left(\frac{\pi d_b^2}{4}\right)n_p n_b \tag{5a}$$

where $k_c = \alpha_{pb}\eta_T v_b(\pi d_b^2/4)$

Considering that the volume of bubbles is conserved, we replace n_b with $\Phi_b/(\pi d_b^3/6)$ yielding a first order rate equation with respect to n_p.

$$\frac{dn_p}{dt} = -\frac{3}{2}\left(\frac{\alpha_{pb}\eta_T v_b \Phi_b n_p}{d_b}\right) \tag{5b}$$

Applying a particle (mass) balance to the contact zone of a DAF tank (see bottom of Fig. 1) for ideal plug flow hydraulics for steady state performance with a contact zone detention time (t_{cz}) yields the performance equation (Eq. (18)) in Table 4. Plug flow is a reasonable approximation for the hydraulics of the contact zone and is discussed in Section 4.3.1.

The modeling approach of Edzwald uses the simple single collector collision efficiency concept in which hydrodynamic interaction and interparticle effects are not considered. These are accounted for by use of α_{pb} – fraction of possible collisions that are successful in attachment. This is discussed further below.

4.3.1. *Discussion of contact zone variables*

The flocculation type models and *white water* blanket model presented above are important contributions. They have increased our understanding of DAF, and they point out important variables affecting design and operation. A brief summary and discussion follow of the variables affecting the contact zone performance with emphasis on those variables identified by the author's model – *white water* blanket model. Note that the model (Eq. (18), Table 4) gives the fraction of particles not attached to air bubbles – whether the particles attached to air bubbles are removed or not in the separation zone depend on their rise velocities, which is addressed later in the paper. Some of the variables are affected by coagulation and flocculation and are referred to as DAF pretreatment variables: these are α_{pb} and η_T. η_T depends on the size of the particles or flocs, which is affected by the flocculation process. Some variables are affected by flotation tank design and operation and are referred to as DAF tank variables: these are η_T (affected by bubble size), Φ_b, v_b, d_b, and t_{cz}.

4.3.1.1. *Pretreatment coagulation.* α_{pb} is the particle–bubble attachment efficiency. In other words, not all of the possible collisions brought about by the particle transport mechanisms yield attachment and removal of particles by bubbles. Thus the single collision efficiency (η_T) is multiplied by the attachment efficiency to account for the overall removal efficiency by a single collector. Conceptually, α_{pb} is the fraction of successful collisions. α_{pb} can have values between 0 (no collisions lead to attachment) and 1 (all collisions result in attachment). Fundamentally, α_{pb} depends on hydrodynamic interaction and interparticle forces as particles approach bubble surfaces. These interparticle forces include electrostatic, van der Waals, and hydrophobic effects. These forces were discussed in Section 4.2.2 and additional comments follow.

Hydrodynamic interaction operates at large separation distances between particles and bubbles. As particles approach bubbles, the water between them must drain away. If there is a resistance to this drainage or thinning of the water layer at the surface, then this affects particle–bubble attachment. This phenomenon is called hydrodynamic interaction or retardation. The single collector collision efficiency terms for interception (η_I) and sedimentation (η_S) show a dependence on d_p^2, although the interception dependence is not exactly this – see Eqs. (15) and (16), Table 4. The power of d_p should be less than 2, if hydrodynamic retardation affects η_I and η_S. Collins and Jameson (1976) found dependence according to $d_p^{1.5}$ indicating a hydrodynamic retardation effect for experiments with polystyrene particles of 4–20 μm particles collected by bubbles of about 50 μm where η_I (interception) is the dominant transport mechanism. On the other hand when settling (η_S) was the main transport mechanism, Reay and Ratcliff (1973) found dependence according to dp^2. It is my assessment that hydrodynamic retardation is more important for larger particles and bubbles acting as rigid solids. It is less important for porous flocs interacting with small air bubbles. It should have a minor effect in DAF, but it would hinder collisions. I consider it conceptually as a physical factor affecting the trajectory of a particle approaching a bubble, and it is accounted for empirically in Eq. (18) by α_{pb}.

Without coagulation, both air bubbles and particles carry negative zeta potentials. When particles approach air bubbles the electrical double layers surrounding the particles and bubbles overlap causing a repulsive force. This is the case for

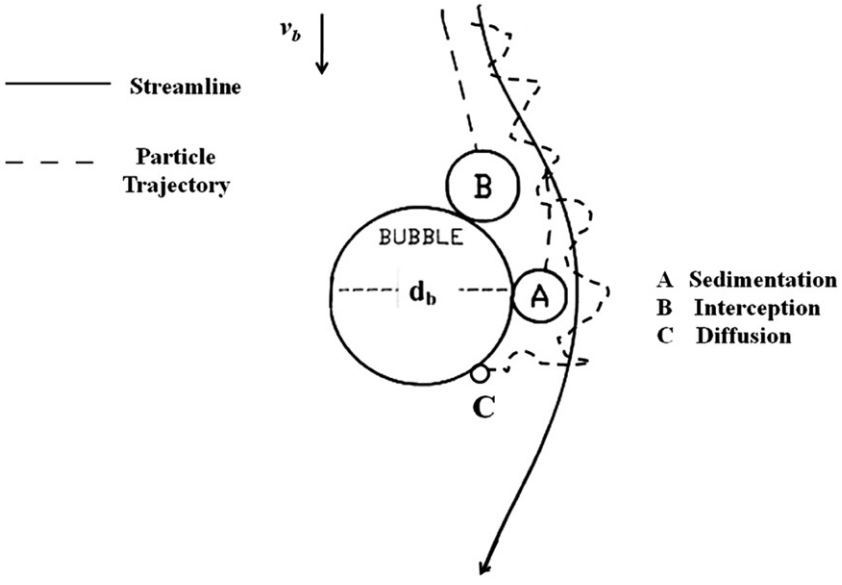

Fig. 4 – Single collector collision efficiency concept for a bubble rising at velocity, v_b, producing streamlines of flow around the bubble (three mechanisms of particle collisions with the bubble are sedimentation, interception, and diffusion; inertia is not important for DAF conditions and not depicted).

no coagulant addition or insufficient coagulant dosing to neutralize the negative charges of particles. It is possible to produce particles and bubbles of opposite charge, which would produce electrostatic attraction. For good coagulation chemistry conditions as practiced for DAF, it is expected that the flocs have little or no electrical charge, so electrostatic forces are low or near zero.

The van der Waals forces between dissimilar particles – i.e., solid particle and an air bubble – may be attractive or repulsive as discussed in Section 4.2.2. If attractive, these forces provide a mechanism for attachment.

The hydrophobic force has to do with bubbles favoring hydrophobic surfaces relative to the water – i.e., the bubbles do not favor being in water and seek a hydrophobic particle surface phase. It is not independent of the other two forces. A reduction in particle charge leads to less electrostatic repulsion so van der Waals forces, if attractive, can become important for the attachment of bubbles. Bubble attachment is favored for hydrophobic particles that are not charged; however, even particles carrying some charge can have hydrophobic spots on the surface that can provide opportunity for bubble attachment. Ducker et al. (1994) made force measurements and found that the hydrophobic force is strong at distances exceeding those associated with double layer interactions, and it is the primary force explaining attachment of hydrophobic particles to air bubbles.

In conclusion, the *white water blanket* model uses the empirical variable α_{pb}. It depends on coagulation pretreatment chemistry (coagulant type, dosage, and pH). With no coagulant addition, the particles carry a negative charge and have some hydrophilic character, so that bubble attachment is poor. Optimum coagulant dosing and pH reduce the particle charge to approximately zero and produces particles with a more hydrophobic character so that attachment to bubbles can occur. The empirical approach for the evaluation of α_{pb} has had success in the use of the Edzwald model. Haarhoff and Edzwald (2004) reported on empirically determined α_{pb} values between 0.5 and 1 for optimum alum coagulation characterized as pH in the mid 6s and dosing yielding flocs of approximately zero charge. Schers and van Dijk (1992) report α_{pb} values of 0.2–1 for six DAF plants in The Netherlands. Shawwa and Smith (2000) found α_{pb} values of 0.35–0.55 for good coagulation conditions. In summary, coagulation is essential in reducing repulsive charge interactions between particles or flocs and bubbles. Favorable attachment (high α_{pb} values) of particles to bubbles requires reduction in the repulsive charge interaction between particles and bubbles. Flocs with zero or low zeta potentials should be produced through coagulation. Under these conditions, attractive forces can prevail (van der Waals or hydrophobic) leading to attachment. Coagulant chemicals are used in water treatment to obtain favorable attachment so α_{pb} depends on coagulation conditions (type, dosage, and pH).

Addition of coagulants can neutralize the charge on particles or flocs so that there is no repulsive force and good attachment conditions occur. This is the case for optimum coagulation conditions of producing flocs with no net charge, and thus the electrostatic force can be ignored for this condition. This is most often the condition of interest in DAF applications. It is possible, although not done in DAF practice, to reverse the charge of the bubble by addition of cationic polymers to the recycle flow leaving saturator. This can produce positively charged bubbles upon injection of the recycle flow into the contact zone. The positively charged bubbles would be electrostatically attracted to raw water negatively charged particles (here, no coagulant added to the main flow). This has been done in experimental systems (Henderson et al., 2008a; Malley, 1995), but it is limited in drinking water applications because metal coagulants are needed to coagulate natural organic matter as well as colloidal particles in water supplies. Han et al. (2006) have also shown that some metal ions at high concentrations and at specific pH conditions can produce positively charged bubbles.

4.3.1.2. Pretreatment flocculation. The purpose of flocculation is to increase the sizes of particles (d_p) so that collection by bubbles in the contact zone is efficient. Fig. 5 compares *white water blanket* model predictions of the contact zone efficiency using Eq. (18) to experimental data as a function of particle size. First, some comments about the experimental data. The experimental data follow generally the model predictions assuming α_{pb} values between 0.5 and 1. The data show an increase in efficiency with increasing particle sizes greater than about 1 μm as predicted by the model. An electronic particle counter was used to measure particles; no particle data are presented for sizes below about 1 μm because the particle counter is unable to measure particles less than this size. The agreement between theory and data is actually good considering that a fixed bubble size of 60 μm was assumed – i.e., the distribution and frequency of bubble sizes were ignored. Furthermore plug flow was assumed, and while this may be a reasonable approximation, there is some dispersion as discussed below.

Additional discussion of the model is warranted. The effect of particle or floc size as shown by the model is discussed first. There is a minimum in the contact zone efficiency for particles with a size of about 1 μm because the single collector efficiency has low values for diffusion, interception, and sedimentation The contact zone efficiency improves with decreasing particle size <1 μm because Brownian diffusion increases as shown by Eq. (14); however, in practice a coagulant would be added causing flocculation of sub-micron particles into larger sizes approaching a micron so additional engineered flocculation is necessary to avoid the minimum in efficiency for 1 μm particles. From Fig. 5 we see that as particle or floc size increases, the contact zone efficiency improves greatly through physical interception – sedimentation is not a significant collision mechanism for low density particles and flocs (here assumed at 1100 kg/m^3). The dependence of η_I (interception) is roughly proportional to the particle size to the second power (d_p^2) – see Eq. (15). If we produce flocs of only about 25 μm, the contact zone efficiency is approximately 99%. An important outcome from the contact zone model predictions is that flocs with sizes of 10's of μm are desired – say, 25–50 μm is optimum. There is agreement by others that high contact zone efficiency occurs for "pin point" size flocs. Mun et al. (2006) report high collision efficiency for the Han model when particle size is similar to bubble size.

This finding of producing "pin point" floc has been incorporated into DAF practice so that flocculation tanks in

DAF plants are designed and operated at much shorter detention times and is discussed further in Section 6. Larger flocs can be produced and floated. In fact, the contact zone efficiency approaches 100% for flocs of large sizes – say 100 μm and greater. However, it is not necessary for good collision opportunities between particles with bubbles since the efficiency is >99% for flocs of 25–50 μm as identified above. In fact, there are some disadvantages in producing large flocs. Detachment of large flocs from bubbles becomes more likely and large flocs require multiple bubble attachment to reduce their density sufficiently to achieve high floc–bubble aggregate rise rates as will be shown in Section 5.

4.3.2. *Discussion of flotation tank variables*

There are five variables affecting DAF contact zone design and operation: bubble size (d_b), single collector efficiency (η_T), bubble rise velocity (v_b), hydraulic contact zone detention time (t_{cz}), and the bubble volume concentration (Φ_b).

Each single collector collision efficiency mechanism depends strongly on bubble size as shown by Eqs. (14)–(16). Each one increases (and thus η_T) with decreasing bubble size (d_b). Furthermore, the denominator of the right hand side of Eq. (18) contains d_b. This also produces an increase in the contact zone efficiency with decreasing bubble size. It is well-known that smaller bubbles are better for flotation, and this is a primary reason why dissolved air flotation is a more efficient process than dispersed air flotation, where bubble sizes are much larger at about 1 mm. It was presented above that bubbles in the contact zone are mainly between 40 and 80 μm in diameter, with a mean bubble size of about 60 μm. While smaller bubbles improve performance just like smaller filter grains improve filtration, the bubble size is fixed mainly by the pressure difference across the recycle injection device and by the injection device (usually nozzles). Therefore the designer insures a good bubble size through the saturator design and nozzle selection, and the operator has little control over bubble size other than to maintain the saturator pressure at the desired level, such as within the range of 400–600 kPa (~60–85 psi).

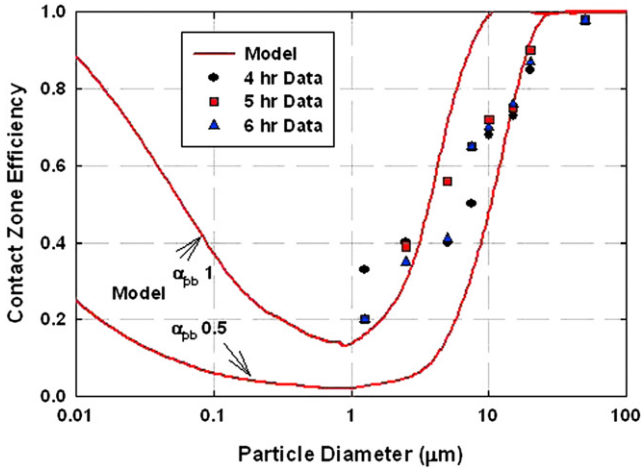

Fig. 5 – Contact zone *white water* blanket model predictions versus experimental data (model assumptions: d_b = 60 μm, ρ_p = 1100 kg/m^3, and α_{pb} of 0.5 and 1; experimental conditions: DAF loading rate 15 m/h, t_{cz} = 1.9 min, T = 5.5 °C, Φ_b = 7840 ppm). Reprinted from Haarhoff and Edzwald (2004). Copyright 2004, with permission from the copyright holders, IWA Publishing.

The bubble rise velocity (v_b) theoretically affects contact zone performance, but practically speaking the designer and plant operator have no ability to control or change. The rise velocity is fixed by the bubble size and water temperature. For 60 μm bubbles, rise velocities are 7 and 4.5 m/h for 20 and 4 °C, respectively.

Increasing the contact zone detention time (t_{cz}) improves the contact zone performance. In practice, the contact zone detention time lies between 1 and 2.5 min for design flow conditions. Haarhoff and Edzwald (2004) have shown through use of the contact zone performance model (Eq. (18)) that the contact zone efficiency is high and insensitive to detention times greater than about 1.5 min. While the contact zone detention time is not varied directly in plant operation, you can expect shorter (design) times in the summer with higher water demands and thus higher flow rates, and longer times in the winter.

In the Edzwald *white water* blanket model (Eq. (18)), ideal plug flow hydraulics is assumed. At the bottom of the contact zone, the recycle flow is introduced by a series of nozzles across the width of the tank. Some think because of this flow injection and the resulting precipitation of air bubbles that there is considerable mixing. However, the nozzles are positioned to produce mixing in the transverse direction to the vertical flow through the contact zone. Consequently there is some dispersion in the axial direction of flow (Shawwa and Smith, 1998), but plug flow is a reasonable approximation as demonstrated by tracer tests done at the pilot-scale by the author. Lundh et al. (2002) made velocity measurements at the pilot-scale across the width and depth of the contact zone. They found mixing at the bottom of the contact zone where air is introduced, but as the water moved away from the bottom toward the top of the contact zone, they found the flow was more like plug flow. For full-scale DAF systems with greater length in the axial direction of flow (i.e., the contact zone depth) than used in pilot-scale, the flow characteristics would be more like plug flow than in pilot-scale systems. Haarhoff and Edzwald (2004) showed that even in considering a reasonable amount of dispersion, the effect on the contact zone efficiency is small and so plug flow is a reasonable assumption.

The most important operating and control variable affecting DAF performance is the bubble volume concentration (Φ_b) in the contact zone. The air concentration can be changed by changing the saturator pressure (dissolving more air into the recycle flow) or by changing the recycle rate – see Table 3. However, the saturator pressure is not varied much so the main operational way to change the bubble concentration is to increase or decrease the recycle flow or ratio (R). The plant operator, as needed, can vary the recycle rate from say 8 to 12% yielding bubble volumes (Φ_b) from about 5900 to 8600 ppm – Table 3. Haarhoff and Edzwald (2004) have shown with the model that contact zone performance is excellent when the bubble volumes exceed about 6000 ppm for a contact zone detention time of at least 1.5 min. Greater bubble volumes yield excellent performance for detention

times as short as 1 min. Poor contact zone performance occurs below 1 min detention time for bubble volumes as high as 9000 ppm.

5. Principles on rise velocities and separation zone clarification performance

> The society which scorns excellence in plumbing as a humble activity and tolerates shoddiness in philosophy because it is an exalted activity will have neither good plumbing nor good philosophy: neither its pipes nor its theories will hold water. John W. Gardner,

I like the above quote from John W. Gardner (writer and former President of the Carnegie Foundation for the Advancement of Teaching) because it is about excellence and uses a metaphor of pipes and theories holding water. The subject of bubble rise velocities is based on sound and straight-forward principles from Stokes. Rise velocities for floc–bubble aggregates require modification of Stokes' law, but determination of the rise velocities is fairly straight-forward. Taking these rise velocities for bubbles and floc–bubble-aggregates and applying it to a DAF tank with continuous flow is also straight-forward, if one assumes an idealized separation zone. Here, we can use the Hazen theory to predict performance for conventional rate DAF systems. Modification of the Hazen theory is required for high-rate DAF systems because the simple vertical ideal flow pattern through the separation zone does not occur.

5.1. *Bubble and floc–bubble aggregate rise velocities*

First we consider the rise rates of bubbles in a column of water under quiescent conditions – no water flow. Stokes' law describes the bubble rise rate for Re $\leq$ 1 according to Eq. (19) in Table 5. It can be argued that the drag coefficient is less for rising air bubbles than for solids and that Eq. (20) can describe bubble rise velocities. Ljunggren et al. (2004) found agreement between predictions with Eq. (20) and measurements for bubbles with sizes of 85 μm and smaller. Nonetheless Eq. (19) is recommended for calculation of rise velocities rather than the slipping condition equation (Eq. (20)) because the latter equation applies to bubbles sizes <100 μm close to the size of interest in the separation zone. Furthermore, Eq. (19) gives lower rise velocities and thus provides a conservative estimate.

Bubbles in the separation zone are larger than those in the contact zone because of coalescence or possibly because of reduced water pressure as the bubbles move from the depth of the contact zone toward to the surface and into the separation zone. For modeling purposes a mean bubble size of 100 μm is assigned; note that this is slightly greater than the bubble sizes commonly found for the contact zone of 40–80 μm – a mean size of 60 μm was used in contact zone modeling. Leppinen and Dalziel (2004) made field observations at full-scale plants and observed bubble sizes smaller and larger than 100 μm for the separation zone (see Table 2), so 100 μm is a reasonable size to use in rise velocity equations. The rise rate for a 100 μm bubble at 20 °C using Eq. (19) is approximately 20 m/h.

Next, rise velocities for floc–bubble aggregates are considered. A summary of model equations are summarized in Table 5. Eq. (21) gives the theoretical rise velocity for floc–bubble aggregates according to Haarhoff and Edzwald (2004) for Re $\leq$ 1. To use the equation requires calculation of a spherically equivalent aggregate diameter (Eq. (22)) and an aggregate density (Eq. (23)) based on the number of attached air bubbles. The *K* in Eq. (21) accounts for the shape of the aggregate and its effect on increased resistance to drag (Tambo and Watanabe, 1979). For small flocs (≤40 μm) attached to bubbles of 100 μm and larger, the aggregate is nearly spherical and *K* is 24. If the flocs are substantially larger than 100 μm bubbles, then the aggregate approaches the floc shape and *K* is 45. Hence *K* is assumed to vary gradually from 24 for flocs of 40 μm and smaller to 45 for flocs of 170 μm.

For transition zone Re of 1–50, the theoretical aggregate rise velocity can be calculated from Eq. (24) according to Haarhoff and Edzwald (2004). The Re exceeds 1 for free bubbles of >125 μm and for aggregates with floc diameter of 160 μm with 4 or more attached air bubbles.

An important point to consider is that the number of bubbles that can attach to one floc is limited. Tambo et al. (1986) formulated Eq. (8) (see Table 4) to determine the maximum number of bubbles (N_{max}) that can possibly attach to a floc. Matsui et al. (1998) consider two cases for predicting aggregate rise velocities. Eq. (25) is used for large flocs with multiple bubble attachment as long as the Re $\leq$ 1. At the other extreme, Eq. (26) is used for flocs smaller than the bubble and allows for multiple flocs attached to each bubble.

Fig. 6 shows aggregate rise velocities for flocs (initial density of 1100 kg/m^3) of varying size with one attached air bubble of 100 μm. For flocs with sizes of 50 μm or less, the aggregate rise velocity is about 20 m/h, which is approximately the same as the rise rate of the same size bubble without an attached floc. The aggregate rise velocity decreases for one bubble attachment to flocs of >50 μm approaching zero (no flotation) for flocs of 200 μm. The figure also shows the effect of multiple bubble attachment for the case of ½ $N_{b,max}$. Aggregate rise rates reach 20 m/h and greater for five and six bubbles attached to flocs of about 200 μm.

Flocs with sizes of 50 μm or less should be prepared for effective removals in the separation zone. These "pin point" flocs have rise velocities of about 20 m/h, which is about the same as free bubbles, and thus represents a maximum rise rate. While larger flocs can achieve these high rise rates, it requires multiple bubble attachment. Considering this finding along with the contact zone theory for optimum floc sizes of 25–50 μm, it is concluded that overall the optimum floc size for flocs entering DAF is 25–50 μm.

5.2. *Separation zone performance*

5.2.1. *Ideal case: conventional rate DAF*

The separation zone design (setting the footprint area) and performance for removal of free bubbles and floc–bubble aggregates are based on Hazen theory, analogous to sedimentation tank theory. Fig. 7 shows an idealized DAF tank.

Table 5 – Rise velocity equations for bubbles and floc–bubble aggregates (equation variables defined at end of paper under Equation Notation).

Equation		Comments	Reference
Bubbles			
$v_b = g(\rho_w - \rho_b)d_b^2/18\mu_w$	(19)	Eq. (19) Stokes Law for laminar flow streamlines around rising bubble, Re $\leq$ 1, holds at 20 °C for $d_b \leq$ 125 μm.	
$v_b = g(\rho_w - \rho_b)d_b^2/12\mu_w$	(20)	Eq. (20) reduced drag on rising bubble due to slipping conditions; holds for Re $\leq$ 1 so for 20 °C for $d_b \leq$ 105 μm.	Clift et al. (1978); Matsui et al. (1998)
Floc–Bubble Aggregates			
$v_{fb} = 4g\left(\rho_w - \rho_{fb}\right)d_{fb}^2/3K\mu_w$	(21)	Eq. (21) for Re $\leq$ 1, holds at 20 °C for $d_{fb} \leq$ 160 μm with 4 attached 100 μm bubbles. K explained in text.	Haarhoff and Edzwald (2004)
where			
$d_{fb} = \left(d_f^3 + N_b d_b^3\right)^{1/3}$	(22)		
$\rho_{fb} = \rho_f d_f^3 + N_b \rho_b d_b^3/d_f^3 + N_b d_b^3$	(23)		
$v_{fb} = (4/3K)^{0.8}\left(g^{0.8}\left(\rho_w - \rho_{fb}\right)^{0.8} d_{fb}^{1.4}/(\rho_w)^{0.2}(\mu_w)^{0.6}\right)$	(24)	Eq. (24) for transition zone Re 1–50.	
$v_{fb} = N_b g \rho_w d_b^3 \varphi^{1/2}/18\mu_w d_{fb}$	(25)	Both equations for Re $\leq$ 1. Eq. (25) applies to case of large number of bubbles attached to each floc.	Matsui et al. (1998)
$v_{fb} = g\rho_w d_b^3 \varphi^{1/2}/18\mu_w \left(d_b^3 + j d_f^3\right)^{1/3}$	(26)	Eq. (26) applies to case of floc size smaller than bubble size and multiple flocs (j) can be attached to each bubble.	

Vertical plug flow is assumed to occur throughout the main part of the separation zone – called the clarification section. The horizontal flow above the baffle separating the contact and separation zones and just below the float (sludge) layer is ignored in evaluating clarification performance. Free bubbles and floc–bubble aggregates are removed if their rise velocities (v_b and v_{fb}) exceed the separation zone hydraulic loading ($v_{sz\text{-}hl}$, which is the downward water velocity for vertical flow) according to Eqs. (27) and (28). Reference values of about 20 m/h for bubble and aggregate rise velocities were presented above. Therefore, these bubbles and aggregates are removed for separation zone hydraulic loadings less than 20 m/h. Conventional rate DAF systems have nominal hydraulic loadings of 5–15 m/h. The separation zone hydraulic loadings (considering only the separation zone footprint area (A_{sz}) and accounting for a recycle rate of 10%) are still less than 20 m/h. Thus, even though plug flow does not occur the hydraulic loadings are conservative enough for conventional rate DAF systems to allow its use for design of the separation zone and to evaluate performance for conventional rate DAF systems.

$$v_b \geq v_{sz-hl} = \frac{Q + Q_r}{A_{sz}} \tag{27}$$

$$v_{fb} \geq v_{sz-hl} = \frac{Q + Q_r}{A_{sz}} \tag{28}$$

For high rate DAF systems in which the hydraulic loadings exceed bubble and aggregate rise velocities, this simple ideal case for modeling the separation zone is inadequate. One must consider the flow path or pattern through the separation zone.

5.2.2. *Flow pattern in the separation zone and stratified flow*

The flow pattern through the separation zone does not follow the simple ideal case of plug flow in the vertical direction. It is influenced by the velocity of water above the baffle (cross-flow velocity), the hydraulic loading, the aspect ratio (length to width ratio), how water is withdrawn at the outlet, and the air bubble suspension in the upper part of the separation zone. There is a concentration difference in bubbles moving from high values near the tank surface and decreasing with depth that produces a density difference affecting the flow pattern. The most extensive work on this subject was done by Lundh et al. (Lundh et al., 2000, 2002; Lundh and Jonsson, 2005). Their research was performed using a pilot-plant and in the 2000 and 2002 papers they used velocity measurements across the length, width, and depth of the separation zone to characterize the flow characteristics. Their 2005 paper used tracer tests. They found that without air bubbles (no injection of the recycle flow) that mixing occurred in the separation zone. A significant finding was that with the presence of air bubbles using typical recycle rates and nominal hydraulic loadings of 10–20 m/h, stratified flow patterns were present in the separation zone. The stratified flow pattern was characterized as horizontal flow near the surface to the far end wall followed by a return horizontal flow immediately below.

A conceptual picture of this stratified flow is shown in Fig. 8. The air bubbles in the stratified zone influence the flow pattern as they create a density difference between the top of the tank where the air bubble concentration is the highest and the bottom of the bubble blanket where the concentration is approaching zero. The bubble blanket penetrates deeper into the tank as the hydraulic loading rate increases and with

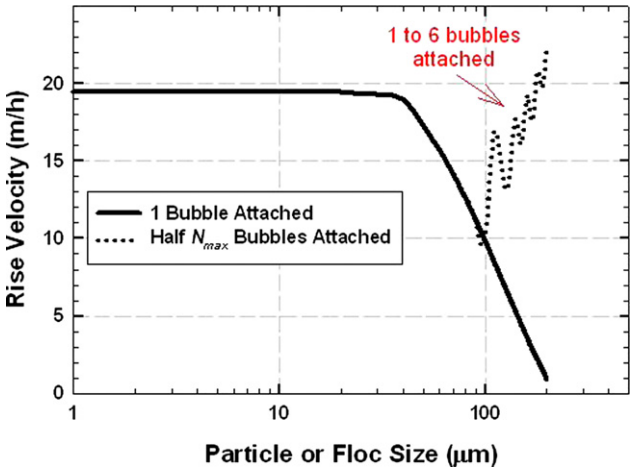

Fig. 6 – Rise velocity of floc–bubble aggregates versus particle size for 1 bubble attachment and multiple bubble attachment (1/2 N_{max}) (conditions: d_b of 100 μm; ρ_f of 1100 kg m^{-3}, 20 °C). Reprinted from Edzwald (2007b). Copyright 2007, with permission from the copyright holders, IWA Publishing.

lower water temperature (Edzwald et al., 1999), and with increasing recycle rate (Han et al., 2009). For DAF tanks with collection of water with pipe laterals across the length of the tank and with porous plate floor type outlets, the water near the bottom of the separation zone moves in a vertical plug flow pattern to the outlet.

Lundh et al. (2002) also reported that the height of the baffle dividing the contact and separation zones affects the flow patterns in the separation zone. If of insufficient height producing too large a distance between the surface and the top edge of the baffle, then a stratified flow pattern did not develop. They suggested that the height should be such that it produces a cross-flow (above the baffle) water velocity of 37 m/h or greater for stratified flow. A cautionary note is that this velocity was obtained from a pilot plant with a set aspect ratio (length to width). Values in design should be based on experience or through computational fluid dynamics – see next sub-section. There is also a limit to the cross-flow velocity in that if it becomes too high (in excess of 100 m/h), it can cause erosion of the floated sludge and deterioration in water quality.

In Section 5.2.1 the separation zone performance for conventional rate DAF was described for an ideal case of simple vertical plug flow and using directly Eqs. (27) and (28). It was discussed that conventional rate DAF systems (nominal hydraulic loadings of 5–15 m/h) have separation zone hydraulic loadings of less than 20 m/h, and so conventional rate DAF systems will perform well since the free bubble and floc–bubble aggregate rise velocities of 20 m/h exceed the separation zone loading rates. For high rate DAF systems, the nominal loading rates are 15–30 m/h (and greater) so the separation zone hydraulic loadings exceed the rise velocities of the bubbles and floc–bubble aggregates. Edzwald (2007b) has used the stratified flow pattern to explain how high rate systems can work. As Edzwald reports, the stratified flow pattern increases the area for clarification and is in accordance with Hazen theory. It is analogous to inserting trays in a sedimentation tank. Using Fig. 8 to illustrate, the horizontal flow near the top of the tank provides a certain clarification area (length times width of the separation zone), which is doubled with the return flow, and then finally tripled with the vertical flow toward the bottom. If one has three flow paths like this, then the clarification hydraulic loading is 1/3 the separation zone loading. In other words, a separation zone loading of say 30 m/h reduces to 10 m/h in terms of the Hazen clarification loading. This clarification loading rate of 10 m/h is less than the expected rise velocities and explains why high rate systems work. Additional material on high rate flotation is presented in Section 7.2.

5.2.3. *Computational fluid dynamics (CFD)*

Computation fluid dynamics (CFD) is a useful design tool to show how velocities within the DAF tank change as a function of flow rate, size of the tank, aspect ratio, baffle height, and

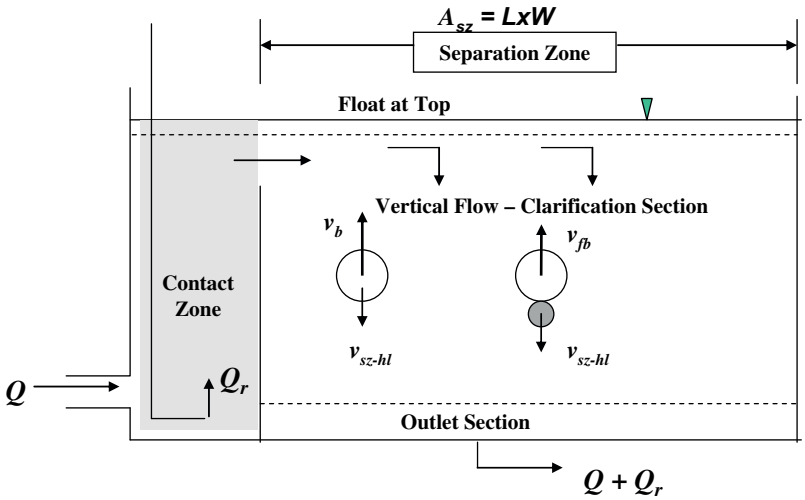

Fig. 7 – Idealized DAF tank showing separation zone divided into three sections: float or sludge layer, vertical flow section for clarification, and the outlet.

water temperature. In some cases it has been used to model water velocities for one phase, water. It is more useful when used to model two phases of water and air bubbles since the air bubble concentration significantly affects the flow patterns and velocities of the water. Several papers have reported on the utility of CFD as a design tool – see Fawcett (1997), Ta and Brignall (1997), Ta et al. (2001), and Amato and Wicks (2009). Amato and Wicks (2009), for example, show how CFD was used to evaluate a plant expansion of increasing the flow through an existing DAF tank and the effect of the baffle height on water velocities and bubble concentrations in the separation zone.

While CFD is a useful design tool, there has been a lack of validation of the model predictions for the presence of two (water and air) and three phases (water, air, and particles). Assumptions have to be made about the bubbles; for example, the bubble size which significantly affects the predictions. Furthermore in practice, particles (solid phase) are present that affect the velocity predictions and air bubble concentrations. Due to the difficulty of including the solid phase, it is usually not included. The presence of the coagulant also affects the flow patterns and position of the bubble blanket, which is ignored in CFD modeling.

6. Laboratory, pilot-plant, and full-scale plant performance

> The test of all knowledge is experiment. Richard P. Feynman

There is a considerable body of experience demonstrating the ability of DAF to treat a variety of water quality cases or source water types. This is addressed in this section. Practical aspects of pretreatment coagulation and flocculation are also addressed. Finally some comments are made about the integration of DAF into water plants.

6.1. *Water quality and source water types*

DAF is effective in separating low density particles from waters. It is considered a better particle separation process than settling in treating water supplies with algae, natural color, or low mineral water turbidities. It is also more effective than settling in treating cold waters. Algae are, of course, of low density and following coagulation and flocculation the densities of the flocs containing algae and metal hydroxide precipitated particles are low, not much greater than water density. In coagulating waters with natural color and low turbidity, the flocs consist mainly of metal-humate precipitate and metal hydroxide precipitated particles, all of low density. Low turbidity supplies after coagulation and flocculation produce low density flocs as well.

6.1.1. *Turbidity supplies*

A question often asked is, how high of a raw water turbidity level can be treated effectively by DAF? The answer depends on two factors. First, DAF can separate mineral particles at high levels but would require higher recycle rates to supply sufficient air to lower the floc–bubble aggregate density. So answering the question, we consider typical design conditions for delivered air at 10–12 mg/L in the contact zone. If mineral turbidity is quite high, then additional air may be required. The second factor has to do with the nature of the turbidity. Is the turbidity non-mineral (organic matter such as algae) or mineral (silts and clays)?

In some older pilot-scale work conducted in England, Rees et al. (1979) showed that DAF could treat a turbid river supply with turbidities up to 100 ntu. The nature of the turbidity was not identified, but being a river supply the high turbidity events would be associated with runoff and ought to have been of mineral nature. Edzwald et al. (1992) conducted a systematic laboratory bench-scale study in which they examined the flotation of clay (montmorillonite) suspensions at 20 and 100 mg/L. The clay particles were small in size, and did not scatter much light so turbidities were 2 and 10 ntu.

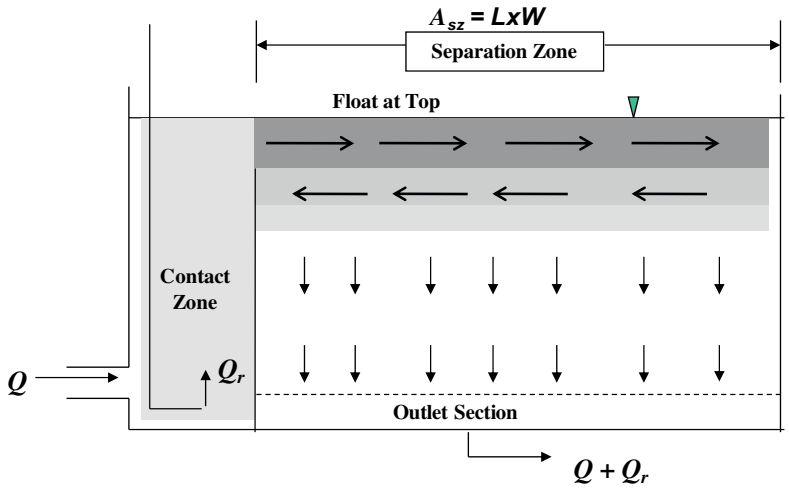

Fig. 8 – Conceptual horizontal stratified flow pattern near the top of the separation zone and vertical plug flow below the bubble blanket. Reprinted from Gregory and Edzwald (2010). Copyright 2010, with permission of the McGraw-Hill Companies.

While the turbidities were not high due to the size of the clay, the mass concentrations are quite high for water supplies. Flotation was effective in reducing the turbidities to less than 1 ntu with 8 percent recycle and saturator pressure of 480 kPa. Han et al. (2003) used kaolin clay with raw water turbidities of about 100 ntu or less in laboratory bench-scale experiments. They obtained good DAF performance with floated water turbidities of 1 ntu.

An important recent study examined 400 water plants in the USA and Canada and examined treatment processes used in the plants against raw water quality (Valade et al., 2009). From the data the authors proposed process selection guidelines with respect to raw water quality. For raw water turbidity, the authors distinguished between mineral and non-mineral turbidity. Fig. 9 shows their process selection diagram based on average raw water quality. The figure shows that DAF is recommended for average raw water mineral turbidity supplies of 10 ntu or less. These supplies are usually river types. DAF is recommended for reservoir type supplies with non-mineral turbidity of 100 ntu or less. The paper also provides guidelines for maximum raw water quality: DAF is recommended as long as the maximum mineral turbidity is <50 ntu and maximum non-mineral turbidity is <200 ntu. Raw water TOC or true color is not a factor in process selection for DAF as it is effective in treating low and high TOC waters.

6.1.2. *Removals of algae*

DAF is more effective than sedimentation in removing algae. This is an important advantage since poor removal of algae can lead to clogging of granular media filters and short filter runs. While diatoms are well-known filter clogging algae, other algae types can clog filters including green algae, flagellates, and blue–green algae (Cyanobacteria).

Edzwald and Wingler (1990) ran systematic laboratory studies using *Chlorella vulgaris* (green algae) and *Cyclotella sp.* (diatom). In side-by-side experiments comparing DAF to sedimentation, they reported 99–99.9% removals by DAF compared to 90–99% by sedimentation. Edzwald et al. (1992) using pilot-scale DAF found 99.9% or greater removal of *Asterionella* (diatom) from a reservoir supply.

Full-scale plant evaluations in the Netherlands have shown the ability of DAF to remove a variety of microorganisms (van Puffelen *et al*, 1995). *Microcystis aeruginosa* and *Oscillatoria aghardii* (both are Cyanobacteria) are the main algae causing problems in the Netherlands water supplies. Vlaški et al. (1996) conducted pilot studies and demonstrated the ability of DAF to remove these Cyanobacteria.

Recent laboratory studies were reported by Teixeira and Rosa (2006, 2007) comparing DAF to sedimentation for removal of blue–green algae (Cyanobacteria). Removal efficiencies by DAF were 92 (or greater) to 98% while sedimentation achieved 70–94%.

A good summary of the effectiveness of DAF with some comparisons to sedimentation can be found in Gregory and Edzwald (2010). Generally, they report 90–99% removal by DAF of algal cells for various algae types compared to 60–90% by sedimentation. A review paper on separation of algae by Henderson et al. (2008b) report DAF removals of 96 to about 99.9% when pretreatment and DAF are optimized.

It is concluded that DAF removes about 90–99% of a variety of algae from water supplies and is more effective than sedimentation. It is noted that when algae levels are exceedingly high, one can expect even greater removals, but when algae levels are low the percent removals are less.

6.1.3. *Removals of Giardia and Cryptosporidium*

Several papers have reported on the performance of DAF in removing protozoan cysts from water. The earliest reported study on removals of *Cryptosporidium* oocysts was by Hall et al. (1995). In flotation jar test type experiments they found for optimum coagulant dosing DAF removals of 85% (0.82 log) to 99.9% (3 log) depending on coagulation pH and coagulant type. In pilot-scale experiments, their oocyst removal data are reported for the combination of DAF and filtration. They found overall removals of about 3 log. It is noted that log removals depend on the spiked or raw water concentrations. If the oocyst concentration is not high and you find below detection levels in the treated water, which is almost always the case with oocyts in filtered waters with optimum coagulation, then the log removals reflect your raw water level. We can gain some additional insight on the ability of DAF by examining additional work, especially research that reports removals by DAF alone and the combination of DAF and filtration.

Plummer et al. (1995) found >2 log removal of *Cryptosporidium parvum* oocysts by DAF alone using bench-scale DAF equipment. Edzwald and Kelley (1998) conducted pilot-plant studies in which they evaluated the removals of *C. parvum* oocysts by DAF alone and by the combination of DAF and dual media filtration. They found, for optimum ferric chloride coagulation, 3 log removals by DAF and a total of 5 log by DAF and filtration. In experiments with alum for optimum coagulation, they found 2 log removals by DAF and a total of 5 log removals by DAF and filtration.

Edzwald et al. (2000) ran pilot studies in which they investigated the removals of *Giardia lamblia* cysts and *C. parvum* oocysts. The experiments were done under challenge conditions of pulse spiking the cysts (310–3700/L) and oocysts (2800–11,000/L) at high concentrations. They ran side-by-side experiments comparing DAF to plate settling alone and the cumulative removals with dual media filters. For optimum coagulation conditions that produced low DAF turbidities (~0.7 ntu) and good filtered water quality (turbidity <0.1 ntu and particle counts (2–15 μm size) of about 10–100 particles/mL (higher for winter water temperatures) yielded high removals of cysts and oocysts. For plate settling the optimum coagulation conditions yielded relatively good performance but not as good as DAF. Plate settling turbidities were 0.7–0.9 ntu, but filtered water turbidities were the same as for the DAF treatment train at <0.1 ntu. Particles counts (2–15 μm) were lower in the DAF effluent compared to plate settling. Given that DAF performed better in terms of particle and turbidities, it is expected and was found that DAF performed better in removing *Giardia* and *Cryptosporidium*. DAF removals for late spring water temperatures (13–14 °C) were 2.8 ± 0.3 log for *Giardia* and 2.5 ± 0.3 log for *Cryptosporidium*. Removals by plate settling were less: 1.45 ± 0.3 log for *Giardia* and 1.4 ± 0.3 log for *Cryptosporidium*. For winter water temperatures (2–3 °C), removals were less than for late spring, but DAF again performed better than plate settling: DAF removals were

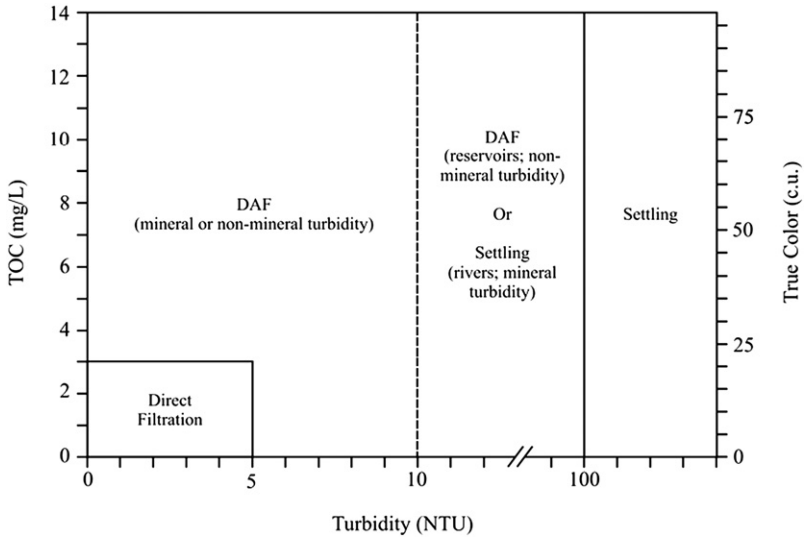

Fig. 9 – Process selection based on average raw water quality for direct filtration, dissolved air flotation plants, and sedimentation plants. Reprinted from Valade et al. (2009). Copyright 2009, with permission from the copyright holders, IWA Publishing.

2.0 ± 0.3 log for *Giardia* and 1.7 ± 0.3 log for *Cryptosporidium*, while plate settling removals were 0.76 ± 0.3 log for *Giardia* and 0.62 ± 0.3 log for *Cryptosporidium*. For both seasons, cumulative removals by DAF and filtration or plate settling and filtration were the same at least 5 log.

Additional pilot-plant experiments were run by Edzwald et al. (2003) examining *C. parvum* removals spiked continuously over about 20–24 h (filter run duration) at concentrations depending on the season: for summer experiments at 17–18 °C, the raw water oocysts concentrations were about 20–40/L; for winter experiments at 2–5 °C, the raw water oocysts concentrations were about 80–160/L. DAF achieved 2 log removals for summer and winter. Plate settling performed well for summer temperatures at slightly less than 2 log removal, but only achieved 1 log removal in the winter. These winter results showing better DAF performance than plate settling were in agreement with turbidity and particle count data in which lower turbidities and particle counts were observed for DAF in contrast to plate settling. Overall *Cryptosporidium* log removals by clarification and dual media filtration were 4–5 for both the DAF and plate settling trains.

In summary DAF is more effective than sedimentation in removing *Giardia* cysts and *Cryptosporidium* oocysts. For design hydraulic loadings, conventional rate DAF can achieve 2–3 log removals compared to removals by sedimentation of 2 log decreasing to 1 log or less for winter water temperatures. An advantage for DAF plants is filtration serves as a polishing step since most of the pathogens are removed by DAF and leave the system in the floated sludge as opposed to leaving in waste filter backwash water.

6.1.4. *Integration of DAF into a water treatment plant*

DAF can be used as a clarification process in a conventional type water plant as depicted at the top of Fig. 1 or as a pretreatment process in membrane plants. The discussion here focuses on the conventional type of plant, which is the most common application of DAF. DAF performance depends on coagulation and flocculation pretreatment. In turn, DAF performs better than sedimentation in removing particles (turbidity) so it affects filtration performance.

Good coagulation chemistry is essential to obtain favorable particle attachment to bubbles. Prior discussion of the fundamentals was presented in Section 4.3.1. Coagulation chemistry is the most important operating control variable affecting flotation performance. Without coagulation, the particles carry a negative charge and are often hydrophilic so that bubble attachment is poor. Good coagulation chemistry depends on coagulant dose and pH. Optimum coagulation conditions are those of coagulant dose and pH that produce flocs with charge near zero and those that produce flocs with relatively high hydrophobicity. These optimum coagulation conditions cause high bubble attachment efficiency.

Flocculation is an important pretreatment process, but it has a different goal than pretreatment flocculation for sedimentation plants. This is an important factor in the integration of DAF into water plants. In settling processes, the goal is to produce flocs with sizes of 100 s of μm. Flocs with these sizes yield settling rates that can be removed for the overflow rates used by conventional and high rate (tube and plate settling) sedimentation processes. For DAF, flocs do not need to be as large since we wish to float the floc–bubble aggregates. In the theory sections for the contact zone (Section 4.3) and for the separation zone (Section 5.1), optimum floc sizes of 25–50 μm were identified. The theory has been supported through bench-scale (Edzwald et al., 1990, 1992; Edzwald and Wingler, 1990; Edzwald, 1995) and pilot-plant data (Edzwald et al., 1992, 1999; Valade et al., 1996). These studies demonstrated that pretreatment flocculation times of 5–10 min are adequate. As a result of these studies and pilot-plant work done in designing DAF plants, the flocculation times for full-scale DAF plants have decreased from 20 to 30 min for plants designed in the 1960s and 1970s to about 10 min at the present time as was discussed in Section 2.2.2 and shown in Fig. 2. In some cases lower flocculation times may be used if demonstrated by pilot studies. An

example is the Croton water plant for New York City, which is a 1100 Ml/d facility with 2-stage flocculation prior to DAF with a total detention time of 5 min (Crossley and Valade, 2006). Pilot studies showed that good performance can be achieved for this water supply with this low flocculation time.

In conclusion, the goal of flocculation for DAF plants is to produce small "pin point" flocs of about 25–50 μm. Flocculation times of about 10 min are recommended, which are much less than for sedimentation plants.

DAF is more effective in removing particles and turbidity than sedimentation processes. Lower particle counts applied to conventional rate filters (say 10–15 m/h) will produce longer filter run times and less frequent backwashing. If DAF is being integrated into new plants, than the lower particle counts and turbidity applied to the filters can be considered in evaluating high rate filtration. A measure of the filtered water production is the unit filter run volume (UFRV), which is the volume of water in m^3 produced in a run divided by the filter area in m^2. A minimum value of 200 m^3/m^2 is used for guidance of effective filter design and operation (MWH, 2005) – a value lower than this indicates the filters are being backwashed too frequently (i.e., short filter runs). Direct filtration plants could operate at this minimum value, but plants with sedimentation should have higher values, say 400 m^3/m^2. Considering DAF is more effective in reducing particles applied to the filter, then even greater UFRVs should be obtained. There have been several pilot studies done for large new DAF water plants demonstrating high UFRVs. Pilot studies done for Boston (Shawcross et al., 1997) found UFRVs of 800 m^3/m^2 and greater. Pilot studies collected for Canada's largest DAF plant (Winnipeg) found UFRVs of about 600 m^3/m^2 (Pernitsky et al., 2007). The full-scale plant was commissioned in late 2009. Pilot-plant data collected in treating the Croton water supply for New York City for summer flow rate loadings showed that UFRVs of 800 m^3/m^2 could be obtained (Nickols et al., 2000).

An extensive evaluation over an entire year of a full-scale DAF plant in Fairfield, CT (USA) was reported by Edzwald and Kaminski (2009). The plant has a capacity of 190 Ml/d, and it is a flotation over filtration plant with a nominal design DAF and filter loading of 15 m/h with dual media filters. The DAF process performed well over the year period with DAF turbidities generally less than 0.4 ntu. Excellent filtered water performance was achieved with average turbidities of 0.07 ntu. High water production was obtained with an average UFRV for the year of 640 m^3/m^2. Even greater UFRVs could be achieved by the plant if the filters were run longer, but filters are backwashed on a schedule basis at night when power costs are less.

In summary, the integration of DAF into conventional type water plants can yield high water production with UFRVs of 600–800 m^3/m^2.

7. State of the technology

> I was taught that the way of progress was neither swift nor easy. Marie Curie

DAF is a relatively new drinking water treatment technology having its roots in Sweden and Finland in the 1960s and gradually spreading to other countries. It is the nature of the drinking water field to be conservative in adapting technologies. The water field requires considerable demonstration of the technology through extensive pilot-plant testing and full-scale plant experience before general acceptance. DAF is now accepted as an effective clarification process in treating a variety of water types, especially reservoir supplies and waters with algae, natural color and low mineral turbidity. Haarhoff (2008) conducted a survey and found some 62 large capacity DAF plants (defined as 50 Ml/d or greater) in 18 countries. The actual number of large plants is undoubtedly larger since the survey was unable to account for all facilities around the world. The author estimates that there are about 150 DAF plants of all sizes in North America alone.

DAF may be placed in a horizontal configuration separate from filtration in a conventional type water treatment plant as depicted at the top of Fig. 1. However, another configuration places flotation over filtration in a vertical configuration – this is discussed further below. In both of these configurations, DAF is used in a conventional type water plant replacing sedimentation ahead of granular media filters. DAF can be used in other type applications as a pretreatment clarification process prior to membranes such as ultrafiltration or in reverse osmosis (RO) desalination. An example of the latter case is the desalination plant in Singapore that went on-line in 2005 (Huijbregsen et al., 2005). Some desalination plants in the Mediterranean and Middle East use DAF for pretreatment. The author predicts expanding use of DAF in pretreatment for ultrafiltration membranes and in RO plants.

7.1. *Flotation over filtration*

Flotation can be placed above the filter in a vertical arrangement in what is called simply, flotation over filtration. Some give it the abbreviated name DAFF and others DAF/F. The process was developed by Purac AB (Sweden) in the 1960s (Crossley and Valade, 2006). It was used for many years in package plants with capacities of 4 Ml/d or lower. DAF/F has the advantage of reducing a water plant's footprint so in the last 15 years we are seeing it used for large water plants. Some examples are the 190 Ml/d plant in Fairfield, CT (USA) that has been operating since 1995 (see Section 6.1.4), the 1100 Ml/d plant for New York City scheduled to go on-line in 2011. Interestingly, the 136 Ml/d Tuas desalination plant for Singapore, mentioned above, uses DAF/F.

Water plants with DAF/F have a smaller plant footprint thereby reducing the land area, which is a significant advantage for large cities. There is also a construction cost savings of having one structure for flotation and filtration compared to conventional rate plants with a horizontal layout of separate units. DAF/F plants do have a couple of disadvantages. One is the filtration and DAF loading rates cannot be independently designed and operated. Since one does not want to design filters at too high a rate, the filters control the hydraulic loading which for DAF/F systems is typically 10–15 m/h. This excludes the use of high rate DAF systems. Another disadvantage with DAF/F is that other processes cannot be placed between flotation and filtration; e.g., an ozone contactor. Application of chemicals between flotation and filtration is also challenging.

A unique version of flotation over filtration is the CoCoDAFF™ process developed in the UK in the early 1990s (Eades and Brignall, 1995; Eades et al., 1997). CoCoDAFF™ is a counter-current process in which the recycle flow from the saturator is introduced above the filter media The flocculated water is introduced above the recycle so that the water flows downward toward the filter media, the air bubbles are rising yielding the counter-current flow feature. Because it is a DAF/F configuration, hydraulic loading rates are controlled by the filters and facilities are designed to 10–15 m/h.

7.2. *High rate DAF systems*

Fig. 2 presented previously in Section 2.2 shows the trend in DAF loading rates with conventional rate systems increasing from 5 m/h in the late 1960s and early 1970s to rates of 10–15 m/h in recent years. High rate systems are a recent development. Edzwald et al. (1999) using a pilot-plant, designed actually for conventional rate DAF use, showed that it could be operated at high rates and achieve good turbidity and particle count performance without adversely affecting filtration performance. In the late 1990s and in the early 2000s, several companies introduced high rate DAF systems at nominal loading rates of 15–30 m/h and greater, many at 20–40 m/h. The nominal loading rate is defined as the treated water flow divided by the gross footprint area (treated water flow excludes the recycle flow and the gross footprint area includes the contact and separation zones).

One system was developed by Rictor Oy (Finland), and it is used by many drinking water plants. The Rictor technology is available around the world by license to Infilco Degrémont, and it is known by the trade name of AquaDAF®. A large plant (Haworth plant in northern New Jersey) with a capacity of 760 Ml/d began operation in June 2009. A key feature of the DAF tank for the AquaDAF® process is the orifice plate floor at the bottom of the DAF tank that produces good flow distribution in the separation zone and at the outlet through the plate floor.

There are other high rate DAF systems. One is available from IIT WWW (Leopold, USA) under the name Clari-DAF™. Amato et al. (2001) and Dahlquist and Göransson (2004) reported on the development by Purac Ltd. (UK) and Purac AB of a high rate DAF process, called DAFRapide®. Additional development has taken place and Enpure (UK, formerly Purac Ltd) has a high rate system under the name of Enflo-vite®.

7.3. *Design and operating parameters*

Table 6 summarizes common design and operating parameters for conventional rate DAF systems. It is presented as a resource and to provide some guidance for those interested in typically used parameters. These parameters are the same for high rate systems for pretreatment flocculation, for the recycle and saturator systems, and for the removal of the floated sludge. What differs, of course, is the DAF tank size and loading rate. DAF tanks for high rate systems are also a little deeper and tend to have a smaller length to width ratio.

8. Research needs

> If we knew what we were doing, it wouldn't be called research, would it? Albert Einstein.

Einstein's statement summarizes quite well what research is about. As research progresses on a subject, we learn two things: what we know and what we do not know. The former improves our understanding of the subject by laying out principles and models. The latter should indentify research needs. Below is my list of research needs for DAF for drinking water. It contains both fundamental and applied research. I am hopeful it will stimulate study and give us a better understanding of DAF. I am also hopeful that DAF, when integrated with other water treatment processes, will provide the field with economical production of drinking water around the world.

8.1. *Bubble production and energy*

The energy required to produce air bubbles depends on the saturator pressure and recycle rate, but the pressures and recycle ratios used for DAF have not changed much since the 1960s. This energy requirement is a significant operating cost. Research is needed on more energy efficient methods to produce the microbubbles used in DAF.

8.2. *Bubble–bubble interaction*

There are four forces that affect bubble–bubble interaction: London-van der Waals, electrostatic, hydrophobic interaction, and hydrodynamic retardation. Research on the effect of ionic strength (0.001–0.68 M (seawater level) on these forces and bubble–bubble interaction would be useful in explaining bubble size stability and any tendency for coalescence.

8.3. *Bubble–particle interaction*

The same four forces as listed above influence bubble–particle interaction. Some investigators account for these forces in an empirical attachment efficiency factor (α_{pb}), while others attempt to write equations for three of the forces (van der Waals, electrostatic, and hydrodynamic retardation) and ignore the hydrophobic force. They consider van der Waals as an attractive force, but others point out that for bubble–particle interaction in water, van der Waals may be repulsive. Another problem is the hydrodynamic interaction equation applies to two solid particles, when we actually have porous flocs interacting with bubbles. Ionic strength can affect bubble–particle interactions, especially when considering DAF for seawater pretreatment. Research is needed on these subjects.

8.4. *Contact zone modeling*

First, what are the hydraulic flow patterns through the contact zone? A case is made in the review that plug flow is a reasonable assumption for modeling purposes. We model many processes as plug flow knowing that some dispersion occurs – e.g., granular media filtration. It would be beneficial to gather evidence on the flow pattern and degree of dispersion as

Table 6 – Design and operating parameters for conventional rate DAF plants.

Item	Values	Comments
Pretreatment flocculation		
Mean detention time (min)	10–20	Some as low as 5 min
Number of stages	2	Some with 3 stages
Mixing intensity (G) (s^{-1})	50–100	Some as low as 30 and some as high as 150 sec^{-1} Propeller or gate flocculators used Some use of tapered flocculation Some use of hydraulic flocculation
DAF Tank		
Nominal hydraulic loading rate (m/h)	5–15	
Separation zone loading rate (m/h)	6–18	Based on the through-put flow and 10% recycle flow, and the separation zone area.
Contact zone detention time (min)	1–2.5	
Basin depth (m)	2.0–3.5	
Recycle and saturator systems		
Air Mass (g/m^3)	6–10	
Recycle rate %	6–12	10% most typical
Saturator gauge pressure (kPa)	400–600	Higher pressures for unpacked saturators
Saturator efficiency (%)	80–95	For saturators with packing; unpacked saturators: 50–70%. Higher efficiencies for higher temperatures.
Floated sludge		
Hydraulic removal	0.5–1% solids	
Chain and flight or reciprocating skimmer	2–3% solids	Some as high as 5%
Beach drum	1–3% solids	Also called star wheel, sludge roller, and flipper

Adapted with permission from Gregory and Edzwald (2010). Copyright 2010, with permission of the McGraw-Hill Companies.

a function of the geometry of the contact zone, the hydraulic loading rate, the recycle flow, and the angle of the nozzles in directing the recycle flow. These data could be collected from tracer studies or by CFD. Second, the boundary between the contact and separation zones is arbitrarily chosen at the baffle dividing these two parts of the DAF tank. However, this is an artificial boundary and collisions and attachment among particles and bubbles most likely occur in the separation zone, especially near the surface and interface with the overlying sludge layer. In this region of the separation zone, there may be bubble coalescence and floc detachment occurring. Research is needed on the extent of collisions and attachment, floc detachment, and bubble coalescence that may occur and how to incorporate these effects into the models.

8.5. *Separation zone modeling*

For conventional rate flotation systems, the ideal flotation tank concept of vertical plug flow through the clarification area of the separation zone is adequate to predict performance. For high rate DAF processes, this ideal theory does not work because the hydraulic loadings can exceed the rise velocities. A stratified flow regime through the separation zone is invoked to explain why high rate systems are able to remove any free bubbles and floc–bubble aggregates. Research is needed on the hydraulic flow characteristics of the separation zone and the stratified flow that occurs; in particular, to incorporate the flow patterns into a performance model.

8.6. *Tastes and odors*

DAF tanks are not designed to strip tastes and odors from water, but stripping does occur and so it is a secondary benefit of DAF treatment. However, I could not find any refereed journal literature that identifies the compounds and quantifies their removals. Research is needed on what compounds are removed, and a model that quantifies their removal in terms of Henry's constants, water and air loadings, bubble size, and any other significant parameters.

8.7. *DAF as a pretreatment process ahead of membranes*

Research is needed on the ability of DAF to serve as pretreatment process with coagulation to remove DOC ahead of microfiltration and ultrafiltration processes and to reduce fouling of ultrafiltration and nanofiltration membrane processes. An area of much needed research, because of the potential of DAF to be a vital integrated process, is DAF as a pretreatment process ahead of desalination by reverse osmosis (RO). DAF is effective in removing algae that can foul RO membranes. Research is needed on the ability of DAF to remove algae and algal polysaccharides and to prevent fouling of RO. The potential of DAF to remove oily wastes that may be present at desalination sites from oil spills also needs to be studied and quantified.

Acknowledgements

The journey described in this paper was rewarding due to the assistance of former graduate students and professional colleagues. These students educated me as much as I educated them, and I am indebted to them for their contributions and friendship: K. Berger, K. Boudreau, D. Bunker, S. Bullock, D. Pernitsky, M. Janay, M. Kelley, M. Mac Phee, J. Malley Jr., S. Olson, W. Parmenter, A. Paralkar, L. Parento, J. Plummer,

C. Yu, B. Wingler, C. Walsh, J. Walsh, C. Tamulonis, C. Udden, and M. Valade. Many professional colleagues have contributed to my DAF journey and I am forever grateful: T. Amato, I. Crossley, J. Dahlquist, H. Dunn, L. Gillberg, R. Gregory, J. Haarhoff, P. Harvey, T. Hedberg, J. Janssens, G. Kaminski, D. Nickols, D. Reckhow, and J. Tobiason.

Equation Notation

a_b: bubble radius
a_p: particle radius
A: gross tank area
A_{sz}: separation zone surface area
C_b: air or bubble mass concentration in the contact zone
C_r: air mass concentration in recycle flow in equilibrium with saturator air at saturator pressure
$C_{s,air}$: air mass concentration at saturation in water for atmospheric pressure
C_{sO}: solubility or equilibrium concentration of oxygen in water for atmospheric air and pressure
Cs_N: solubility or equilibrium concentration of nitrogen in water for atmospheric air and pressure
d_b: bubble diameter
d_{cb}: critical bubble nucleus
d_f : equivalent spherical floc diameter
d_p: particle diameter
d_{fb}: diameter of the floc–bubble aggregate
d_{sd}: separation distance between bubbles
e: efficiency in delivering air
E_{pb}: theoretical collision and attachment efficiency coefficient
g: gravitational constant (9.806 m/s^2)
G: Camp root-mean-square velocity gradient
j: number of flocs attached to an air bubble
k: air deficit concentration
k_b: Boltzmann constant
k_c: second order kinetic rate coefficient
k_T: collision rate coefficient for turbulent fluid motion
K: factor for shape effects on drag
L: separation zone length
n_b: bubble number concentration
n_b': bubble number per time per area
$n_{f,i}$: particle concentration with attached air bubbles i for batch kinetics
n_p: particle concentration for batch kinetics
$n_{p,o}$: particle concentration without attached air bubbles for batch kinetics
n_o: initial particle concentration for batch kinetics
$n_{p,i}$: floc or particle number concentration in the contact zone influent
$n_{p,e}$: floc or particle number concentration in the contact zone effluent
N_b: number of bubbles attached to a floc
$N_{b,max}$: maximum number of bubbles that can attach to one floc
P: pressure
Q: through-put or treated water flow rate
Q_r: recycle flow rate
r_b: bubble radius
r_p: particle radius
R: recycle rate or ratio
t: time
t_{cz}: contact zone hydraulic detention time
v_b: bubble rise velocity
v_{fb}: floc–bubble rise velocity
$v_{clar\text{-}hl}$: clarification area hydraulic loading
$v_{nom\text{-}hl}$: nominal tank hydraulic loading
v_p: particle settling velocity
$v_{sz\text{-}hl}$: separation zone hydraulic loading
v_w: water velocity
W: separation zone width
X_c: critical distance for particle capture
α_{pb}: particle–bubble attachment efficiency
$\alpha_{pb,i}$: particle–bubble attachment efficiency for flocs with i attached bubbles
β_{DS}: collision efficiency function for differential sedimentation
ε: energy dissipation rate per water volume
η_T: total single collector efficiency
η_D: single collector efficiency: Brownian diffusion
η_I: single collector efficiency: interception
η_S: single collector efficiency: settling
μ: water dynamic viscosity
π: mathematical constant (3.14)
ρ_b: air bubble density
ρ_p: particle or floc density
ρ_{fb}: floc–bubble density
ρ_w: water density
σ: surface tension of water
φ: sphericity of the floc–bubble aggregate
Φ_b: air or bubble volume concentration

REFERENCES

Amato, T., Edzwald, J.K., Tobiason, J.E., Dahlquist, J., Hedberg, T., 2001. An integrated approach to dissolved air flotation. Water Science and Technology 43 (8), 19–26.

Amato, T., Wicks, J., 2009. The practical application of computational fluid dynamics to dissolved air flotation, water treatment plant operation, design and development. Journal of Water Supply: Research and Technology – Aqua 58 (1), 65–73.

Bratby, J.R., Marais, G.v.R., 1975a. Dissolved air (pressure) flotation—an evaluation of interrelationships between process variables and their optimisation for design. Water SA 1 (2), 57–69.

Bratby, J.R., Marais, G.v.R., 1975b. Saturator performance in dissolved air (pressure) flotation. Water Research 9 (11), 929–936.

Cassell, E.A., Matijevic, E., Mangravite, F.J., Buzzell, T.D., Blabac, S. B., 1971. Removal of colloidal pollutants by microflotation. AIChE Journal 17 (6), 1486–1492.

Clift, R., Grace, J.R., Weber, M.E., 1978. Bubbles, Drops, and Particles. Academic Press, San Diego, CA.

Collins, G.L., Jameson, G.J., 1976. Experiments on the flotation of fine particles: the influence of particle size and charge. Chemical Engineering Science 31, 985–991.

Craig, V.S.J., Ninham, B.W., Pashley, R.M., 1993. Effect of electrolytes on bubble coalesence. Nature 364, 317–319.

Crossley, I.A., Herzner, J., Bishop, S.L., Smith, P.D., 2007. Going Underground – Constructing New York City's First Water Treatment Plant, a 1,100 Ml/d Dissolved Air Flotation, Filtration, and UV Facility. The 5th International Conference on Flotation in Water and Wastewater Systems Seoul National University, Seoul, South Korea, pp. 143–151.

Crossley, I.A., Valade, M.T., 2006. A review of the technological developments of dissolved air flotation. Journal of Water Supply: Research and Technology – Aqua 55 (7–8), 479–491.
Dahlquist, J., Göransson, K., 2004. Evolution of a high rate dissolved air flotation process – from idea to full-scale application. In: Hahn, H., Hoffmann, E., Ødegaard, H. (Eds.), Chemical Water and Wastewater Treatment. IWA Publishing, London, UK, pp. 297–308.
De Rijk, S.E., Van der Graaf, J., Den Blanken, J.G., 1994. Bubble size in flotation thickening. Water Research 28 (2), 465–473.
Derjaguin, B.V., Dukhin, S.S., Rulyov, N., 1984. In: Matijevic, E., Good, R.J. (Eds.), Surface and Colloid Science. Plenum Press, New York, pp. 71–113.
Dockko, S., Han, M., 2004. Fundamental characteristics of bubbles and ramifications for the flotation process. Water Science and Technology: Water Supply 50 (12), 207–214.
Ducker, W.A., Xu, Z., Israelachvili, J.N., 1994. Measurements of hydrophobic and DLVO forces in bubble–surface interactions in aqueous solutions. Langmuir 10, 3279–3289.
Eades, A., Brignall, W.J., 1995. Counter-current dissolved air flotation/filtration. Water Science and Technology 31 (3–4), 173–178.
Eades, A., Jordan, D., Scheidler, S., 1997. Counter-current Dissolved Air Flotation Filtration COCO-DAFF. Proceedings Dissolved Air Flotation Conference. Chartered Institution of Water and Environmental Management, London, pp. 323–340.
Edzwald, J.K., 1995. Principles and applications of dissolved air flotation. Water Science and Technology 31 (3–4), 1–23.
Edzwald, J.K., 2007a. Fundamentals of dissolved air flotation. Journal of the New England Water Works Association 121 (3), 89–112.
Edzwald, J.K., 2007b. Developments of high rate dissolved air flotation for drinking water treatment. Journal of Water Supply: Research and Technology – Aqua 56 (6–7), 399–409.
Edzwald, J.K., Malley Jr., J.P., Yu, C., 1990. A conceptual model for dissolved air flotation in water treatment. Water Supply 8, 141–150.
Edzwald, J.K., Walsh, J.P., Kaminski, G.S., Dunn, H.J., 1992. Flocculation and air requirements for dissolved air flotation. Journal of the American Water Works Association 84 (3), 92–100.
Edzwald, J.K., Olson, S.C., Tamulonis, C.W., 1994. Dissolved Air Flotation: Field Investigations. American Water Works Association Research Foundation, Denver.
Edzwald, J.K., Tobiason, J.E., Amato, T., Maggi, L.J., 1999. Integrating high rate dissolved air flotation technology into plant design. Journal of the American Water Works Association 91 (12), 41–53.
Edzwald, J.K., Tobiason, J.E., Parento, L.M., Kelley, M.B., Kaminski, G.S., Dunn, H.J., Galant, P.B., 2000. *Giardia* and *Cryptosporidium* removals by clarification and filtration under challenge conditions. Journal of the American Water Works Association 92 (12), 70–84.
Edzwald, J.K., Tobiason, J.E., Udden, C., Kaminski, G.S., Dunn, H.J., Galant, P.B., Kelley, M.B., 2003. Evaluation of the effect of recycle of waste filter backwash water on plant removals of *Cryptosporidium*. Journal of Water Supply: Research and Technology – Aqua 52 (4), 243–258.
Edzwald, J.K., Han, M., 2007. In: Edzwald, J.K., Han, M. (Eds.), The 5th International Conference on Flotation in Water and Wastewater Systems. Seoul National University, Seoul, South Korea, p. 393.
Edzwald, J.K., Kaminski, G.S., 2009. A practical method for water plants to select coagulant dosing. Journal of the New England Water Works Association 123 (1), 15–31.
Edzwald, J.K., Kelley, M.B., 1998. Control of *Cryptosporidium*: from reservoirs to clarifiers to filters. Water Science and Technology 37 (2), 1–8.
Edzwald, J.K., Wingler, B.J., 1990. Chemical and physical aspects of dissolved air flotation for the removal of algae. Journal of Water Supply: Research and Technology – Aqua 39 (2), 24–35.
Fawcett, N.S.J., 1997. The Hydraulics of Flotation Tanks: Computational Modeling, Proceedings Dissolved Air Flotation Conference, pp. 51–71. The Chartered Institution of Water and Environmental Management, London.
Flint, L.R., Howarth, W.J., 1971. The collision efficiency of small particles with spherical air bubbles. Chemical Engineering Science 26, 1155–1168.
Friedlander, S.K., 1977. Smoke, Dust, and Haze. John Wiley and Sons, New York.
Fukushi, K., Tambo, N., Matsui, Y., 1995. A kinetic model for dissolved air flotation in water and wastewater treatment. Water Science and Technology 31 (3–4), 37–47.
Fukushi, K., Matsui, Y., Tambo, N., 1998. Dissolved air flotation: experiments and kinetic analysis. Journal of Water Supply: Research and Technology – Aqua 47 (2), 76–86.
Gregory, R., 1997. Summary of General Developments in DAF for Water Treatment since 1976. Proceedings Dissolved Air Flotation Conference. The Chartered Institution of Water and Environmental Management, London, pp. 1–8.
Gregory, R., Edzwald, J.K., 2010. Sedimentation and flotation. In: Edzwald, J.K. (Ed.), Water Quality and Treatment, sixth ed. McGraw Hill, New York (Chapter 9).
Haarhoff, J., 2008. Dissolved air flotation: progress and prospects for drinking water treatment. Journal of Water Supply: Research and Technology – Aqua 57 (8), 555–567.
Haarhoff, J., Edzwald, J.K., 2004. Dissolved air flotation modeling: insights and shortcomings. Journal of Water Supply: Research and Technology – Aqua 53 (3), 127–150.
Haarhoff, J., Steinback, S., 1996. A model for the prediction of the air composition in pressure saturators. Water Research 30 (12), 3074–3082.
Haarhoff, J., Van Vuuren, L., 1995. Design parameters for dissolved air flotation in South Africa. Water Science and Technology 31 (3–4), 203–212.
Haarhoff, J., van Vuuren, L., 1993. A South African Design Guide for Dissolved Air Flotation. Water Research Commission, Pretoria, South Africa.
Hall, T., Pressdee, J., Gregory, R., Murray, K., 1995. *Cryptosporidium* removal during water treatment using dissolved air flotation. Water Science and Technology 31 (3–4), 125–135.
Han, M.Y., 2002. Modeling of DAF: the effect of particle and bubble characteristics. Journal of Water Supply: Research and Technology – Aqua 51 (1), 27–34.
Han, M., Dockko, S., 1999. Zeta potential measurement of bubbles in DAF process and its effect on the removal efficiency. Water Supply 17 (3–4), 177–182.
Han, M., Dockko, S., Park, C., 1997. Collision Efficiency Factor of Bubble and Particle in DAF. Proceedings Dissolved Air Flotation Conference. The Chartered Institution of Water and Environmental Management, London, pp. 409–416.
Han, M., Park, Y., Lee, J., Shim, J., 2002. Effect of pressure on bubble size in dissolved air flotation. Water Science and Technology: Water Supply 2 (5–6), 41–46.
Han, M., Lee, J., Park, Y., 2003. Assessment of the Treatability of Highly Turbid Water by Dissolved Air Flotation Asian Water Quality Conference.
Han, M., Kim, M.K., Shin, M.S., 2006. Generation of positively charged bubble and its possible mechanism of formation. Journal of Water Supply: Research and Technology – Aqua 55 (7–8), 471–478.
Han, M., Kim, T., Kwak, D., 2009. Measurement of bubble bed depth in dissolved air flotation using a particle counter. Journal of Water Supply: Research and Technology – Aqua 58 (1), 57–63.

Han, M., Lawler, D.F., 1992. The (relative) insignificance of G in flocculation. Journal of the American Water Works Association 84 (10), 79–91.
Heinänen, J., Jokela, P., Ala-Peijari, T., 1995. Use of dissolved air flotation in potable water treatment in Finland. Water Science and Technology 31 (3–4), 225–238.
Henderson, R.K., Parsons, S.A., Jefferson, B., 2008a. Surfactants as bubble surface modifiers in the flotation of algae: dissolved air flotation that utilizes a chemically modified bubble surface. Environmental Science and Technology 42 (13), 4883–4888.
Henderson, R.K., Parsons, S.A., Jefferson, B., 2008b. The impact of algal properties and pre-oxidation on solid-liquid separation of algae. Water Research 42, 1827–1845.
Huijbregsen, C.M., Appan, A., Bhat, G., 2005. Dissolved Air Flotation/filtration Pre-treatment in Seawater Desalination. International Desalination Association – World Congress on Desalination and Water Reuse, SP05-083, Singapore. International Desalination Association, Topsfield, MA.
Israelachvili, J.N., Pashley, R.M., 1982. The hydrophobic interaction is long range, decaying exponentially with distance. Nature 300, 341–342.
Kiuru, H., Vahala, R., 2000. In: Kiuru, H., Vahala, R. (Eds.), Dissolved Air Flotation in Water and Wastewater Treatment. IWA Publishing, p. 210.
Leppinen, D.M., 1999. Trajectory analysis and collision efficiency during microbubble flotation. Journal of Colloid and Interface Science 212, 431–442.
Leppinen, D.M., 2000. A kinetic model of dissolved air flotation including the effects of interparticle forces. Journal of Water Supply: Research and Technology – Aqua 49 (5), 259–268.
Leppinen, D.M., Dalziel, S.B., 2004. Bubble size distribution in dissolved air flotation tanks. Journal of Water Supply: Research and Technology – Aqua 53 (8), 531–543.
Ljunggren, M., Jonsson, L., Jansen, J., 2004. Particle visualization – a tool for determination of rise velocities. Water Science and Technology 50 (12), 229–236.
Longhurst, S.J., Graham, N.J.D., 1987. Dissolved air flotation for potable water treatment: a survey of operational units in Great Britain. The Public Health Engineer 14 (6), 71–76.
Lu, S., 1991. Hydrophobic interaction in flocculation and flotation 3. Role of hydrophobic interaction in particle–bubble attachment. Colloids and Surfaces 57, 73–81.
Lundh, M., Jonsson, L., Dahlquist, J., 2000. Experimental studies of the fluid dynamics in the separation zone in dissolved air flotation. Water Research 34 (1), 21–30.
Lundh, M., Jonsson, L., Dahlquist, J., 2002. The influence of the contact zone configuration on the flow structure in a dissolved air flotation pilot plant. Water Research 36, 1585–1595.
Lundh, M., Jonsson, L., 2005. Residence time distribution characterization of the flow structure in dissolved air flotation. Journal of Environmental Engineering (ASCE) 131 (1), 93–101.
Malley, J.P., 1995. The use of selective and direct DAF for removal of particulate contaminants in drinking water treatment. Water Science and Technology 31 (3–4), 49–57.
Mangravite, F.J., Buzzell, T.D., Cassell, E.A., Matijevic, E., Saxton, G.B., 1975. Removal of humic acid by coagulation and microflotation. Journal of the American Water Works Association 67, 88–94.
Matsui, Y., Fukushi, K., Tambo, N., 1998. Modeling, simulation, and operational parameters of dissolved air flotation. Journal of Water Supply: Research and Technology – Aqua 47 (1), 9–20.
Mun, J., Park, S., Han, M., 2006. Effects of Al^{3+} and hydraulic characteristics on the removal and behaviour of particles in dissolved air flotation. Water Science and Technology: Water Supply 6 (3), 89–95.
MWH, 2005. Water Treatment: Principles and Design, second ed. John Wiley & Sons, Hoboken, NJ.
Nickols, D., Moerschell, G.C., Broder, M.V., 1995. The first DAF water treatment plant in the United States. Water Science and Technology 31 (3–4), 239–246.
Nickols, D., Schneider, O.D., Leggiero, S., 2000. Pilot-testing of high-rate DAF for New York City. Proceedings of the 4th International Conference: Flotation in Water and Waste Water Treatment, Helsinki, Finland.
Offringa, G., 1995. Dissolved air flotation in southern Africa. Water Science and Technology 31 (3–4), 159–172.
Okada, K., Akagi, Y., Kogure, M., Yoshioka, N., 1990. Analysis of particle trajectories of small particles when the particles and bubbles are charged. The Canadian Journal of Chemical Engineering 68 (4), 614–621.
Pernitsky, D.J., Breese, S., Wobma, P., Griffin, G., Kjartansan, K., Sorokowski, R., 2007. From Pilot Tests to Design on Canada's Largest DAF Water Treatment Plant. Proceedings of the 5th International Conference on Flotation in Water and Wastewater Systems. Seoul National University, Seoul, South Korea, pp. 203–210.
Plummer, J.D., Edzwald, J.K., Kelley, M.B., 1995. Removal of *Cryptosporidium parvum* from drinking water by dissolved air flotation. Journal of the American Water Works Association 87 (9), 85–95.
Reay, D., Ratcliff, G.A., 1973. Removal of fine particles from water by dispersed air flotation: effects of bubble size and particle size on collision efficiency. The Canadian Journal of Chemical Engineering 51 (2), 178–185.
Rees, A.J., Rodman, D.J., Zabel, T.F., 1979. Water Clarification by Flotation – 5, TR 114. Water Research Centre, Medmenham, U.K.
Rykaart, E.M., Haarhoff, J., 1995. Behaviour of air injection nozzles in dissolved air flotation. Water Science and Technology 31 (3–4), 25–36.
Schers, G.J., van Dijk, J.C., 1992. Dissolved-air flotation: theory and practice. In: Klute, R., Hahn, H.H. (Eds.), Chemical Water and Wastewater Treatment II. Springer-Verlag, New York, pp. 223–246.
Shawcross, J., Tran, T., Nickols, D., Ashe, C.R., 1997. Pushing the Envelope: Dissolved Air Flotation at Ultra- High Rate. Proceedings Dissolved Air Flotation Conference. The Chartered Insitution of Water and Environmental Management, London, pp. 121–139.
Shawwa, A.R., Smith, D.W., 1998. Hydrodynamic characterization in dissolved air flotation contact zone. Water Science and Technology 38 (6), 245–252.
Shawwa, A.R., Smith, D.W., 2000. Dissolved air flotation model for drinking water treatment. Canadian Journal of Civil Engineering 27, 373–382.
Steinback, S., Haarhoff, J., 1998. A simplified method for assessing the saturation at full-scale dissolved air flotation plants. Water Science and Technology 38 (6), 303–310.
Ta, C.T., Brignall, W.J., 1997. Application of Single Phase Computational Fluid Dynamics Techniques to Dissolved Air Flotation Tank Studies. Proceedings Dissolved Air Flotation Conference. The Chartered Institute of Water and Environmental Management, London, pp. 471–487.
Ta, C.T., Beckley, J., Eades, A., 2001. A multiphase CFD model of DAF process. Water Science and Technology 43 (8), 153–157.
Tambo, N., Matsui, Y., Fukushi, K., 1986. A Kinetic Study of Dissolved Air Flotation. World Congress of Chemical Engineering, Tokyo, pp. 200–203.
Tambo, N., Watanabe, Y., 1979. Physical characteristics of flocs – I. The floc density function and aluminum floc. Water Research 13 (5), 409–419.
Teixeira, M.B., Rosa, M.J., 2006. Comparing dissolved air flotation and conventional sedimentation to remove cyanobacterial

cells of *Microcystis aeruginosa* Part I: the key operating conditions. Separation and Purification Technology 52, 84–94.
Teixeira, M.B., Rosa, M.J., 2007. Comparing dissolved air flotation and conventional sedimentation to remove cyanobacterial cells of *Microcystis aeruginosa* Part II: the effect of water background organics. Separation and Purification Technology 53, 126–134.
Valade, M.T., Edzwald, J.K., Tobiason, J.E., Dahlquist, J., Hedberg, T., Amato, T., 1996. Particle removal by flotation and filtration: pretreatment effects. Journal of the American Water Works Association 88 (12), 35–47.
Valade, M.T., Becker, W.B., Edzwald, J.K., 2009. Treatment selection guidelines for particle and NOM removal. Journal of Water Supply: Research and Technology – Aqua 58 (6), 424–432.
van Puffelen, J., Buijs, P.J., Nuhn, P.N.A.M., Hijen, W.A.M., 1995. Dissolved air flotation in potable water treatment: the Dutch experience. Water Science and Technology 31 (3–4), 149–157.
Vlaški, A., van Breemen, A.N., Alaerts, G.J., 1996. Optimisation of coagulation conditions for the removal of cyanobacteria by dissolved air flotation or sedimentation. Journal of Water Supply: Research and Technology – Aqua 45 (5), 252–261.
Yao, K.M., Habibian, M.T., O'Melia, C.R., 1971. Water and wastewater filtration: concepts and applications. Environmental Science and Technology 5, 1105–1112.
Zabel, T., 1984. Flotation in Water Treatment. Matinus Nijhoff, Boston.